Accepted Manuscript

Antimalarial naphthoquinones. Synthesis via click chemistry, *in vitro activity*, docking to *Pf*DHODH and SAR of lapachol-based compounds

Geraldo Célio Brandão, Franciele C. Rocha Missias, Lucas Miquéias Arantes, Luciana Ferreira Soares, Kuldeep K. Roy, Robert J. Doerksen, Alaíde Braga de Oliveira, Guilherme Rocha Pereira

PII: S0223-5234(17)31067-X

DOI: 10.1016/j.ejmech.2017.12.051

Reference: EJMECH 10029

To appear in: *European Journal of Medicinal Chemistry*

Received Date: 10 September 2017

Revised Date: 11 December 2017

Accepted Date: 13 December 2017

Please cite this article as: Geraldo.Cé. Brandão, F.C. Rocha Missias, Lucas.Miqué. Arantes, L.F. Soares, K.K. Roy, R.J. Doerksen, Alaí. Braga de Oliveira, G.R. Pereira, Antimalarial naphthoquinones. Synthesis via click chemistry, *in vitro activity*, docking to *Pf*DHODH and SAR of lapachol-based compounds, *European Journal of Medicinal Chemistry* (2018), doi: 10.1016/j.ejmech.2017.12.051.

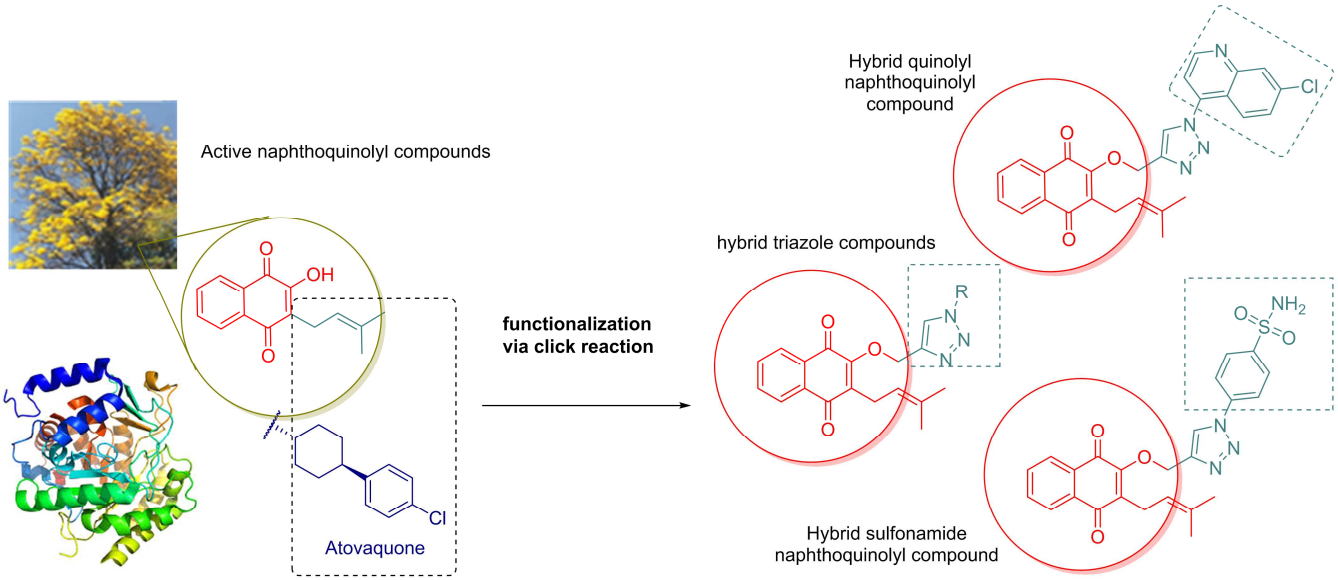

Antimalarial naphthoquinones. Synthesis via click chemistry, *in vitro activity*, docking to *Pf*DHODH and SAR of lapachol-based compounds

Geraldo Célio Brandão[a], *Franciele C. Rocha Missias*[b], *Lucas Miquéias Arantes*[c], *Luciana Ferreira Soares*[c], *Kuldeep K. Roy*[d,e], *Robert J. Doerksen*[d], *Alaíde Braga de Oliveira*[c], *Guilherme Rocha Pereira*,[b,c]*

[a] Departamento de Farmácia, Escola de Farmácia, UFOP, Campus Morro do Cruzeiro, s/n, Balxita, CEP 35400-000, Ouro Preto, MG, Brazil

[b]Pontifícia Universidade Católica de Minas Gerais, PUC Minas, Departamento de Física e Química Instituto de Ciências Exatas e Informática ICEI. Av. Dom José Gaspar, 500 Prédio 34 Coração Eucarístico - CEP 30535.901, Belo Horizonte, MG Brazil

[c]Departamento de Produtos Farmacêuticos, Faculdade de Farmácia, UFMG, Av. Antônio Carlos, 6627, Campus Pampulha, CEP 31270-901, Belo Horizonte, MG, Brazil.

[d]Department of BioMolecular Sciences and Research Institute of Pharmaceutical Sciences, School of Pharmacy, University of Mississippi, University, MS, USA.

[e]National Institute of Pharmaceutical Education and Research, 4, Raja S. C. Mullick Road, Jadavpur, Kolkata 700 032, WB, India.

KEYWORDS malaria, atovaquone, *Plasmodium falciparum*, copper-catalyzed cycloaddition, triazole, chloroquine, dihydroorotate dehydrogenase (DHODH).

ABSTRACT

Lapachol is an abundant prenyl naphthoquinone occurring in Brazilian Bignoniaceae that was clinically used, in former times, as an antimalarial drug, despite its moderate effect. Aiming to search for potentially better antimalarials, a series of *1,2,3*-triazole derivatives was synthesized by chemical modification of lapachol. Alkylation of the hydroxyl group gave its propargyl ether which, via copper-catalyzed cycloaddition (CuAAC) click chemistry with different organic azides, afforded 17 naphthoquinonolyl triazole derivatives. All the synthetic compounds were evaluated for their *in vitro* activity against chloroquine resistant *Plasmodium falciparum* (W2) and for cytotoxicity to HepG2 cells. Compounds containing the naphthoquinolyl triazole

moieties showed higher antimalarial activity than lapachol (IC_{50} 123.5 μM) and selectivity index (SI) values in the range of 4.5 to 197.7. Molecular docking simulations of lapachol, atovaquone and all the newly synthesized compounds were carried out for interactions with *pf* DHODH, a mitochondrial enzyme of the parasite respiratory chain that is essential for *de novo* pyrimidine biosynthesis. Docking of the naphthoquinonolyl triazole derivatives to *pf*DHODH yielded scores between -9.14 and -14.55 units, compared to -9.137 for lapachol and -12.95 for atovaquone and disclosed the derivative **17** as a lead compound. Therefore, the study results show the enhancement of DHODH binding affinity correlated with improvement of SI values and *in vitro* activities of the lapachol derivatives.

1. Introduction

Malaria remains a serious parasitic disease in tropical areas due to its high morbidity and mortality rates. It is estimated that 212 million cases occurred globally in 2015, leading to 429, 000 deaths, most of which were in children aged under 5 years in Africa [1, 2]. The protozoans *Plasmodium falciparum* and *P. vivax* are the main parasites responsible for this disease; the former, the most virulent, is responsible for 99% of the deaths. Resistance to antimalarial drugs has been observed as a consequence of genetic mutations and is a serious setback to antimalarial programs, since it limits the use of effective drugs like chloroquine [3] and artemisinin [4]. Therefore, discovery of new categories of antimalarial lead compounds is an important priority [5].

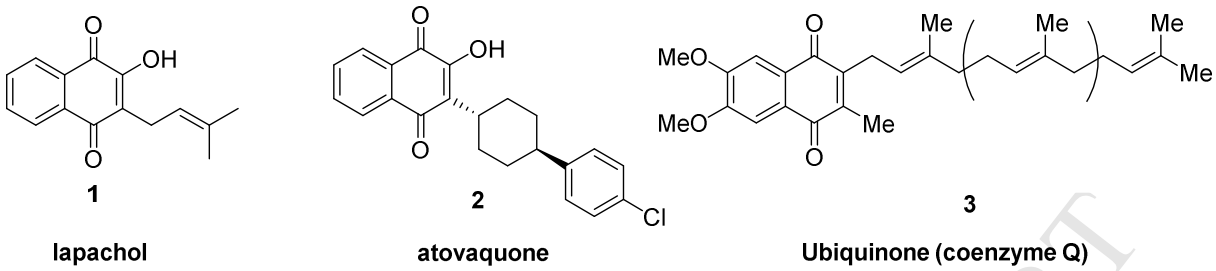

Figure 1. *Chemical structures of lapachol (1), atovaquone (2) and ubiquinone (3).*

Quinones represent a large and important class of carbonyl-conjugated cyclic compounds with a great number of therapeutic applications. Naturally-occurring naphthoquinones are commonly found throughout different plant families, fungi and certain animals [6]. In this project, we started with lapachol (**1**) because it is a well-known antimalarial compound. Lapachol is a hydroxy-prenyl naphthoquinone occurring in woody trees of South American Bignoniaceae [5]. Lapachol has been studied as an interacting molecule with various protein targets such as plasmodial HSP70, [7] though in many studies its detailed mechanism of action is unknown and/or unreported [8]. It has been shown to interact with DHODH, but much more strongly with human DHODH (1 nM) than with PfDHODH (16 μM) [9]. Other modified lapachols, such as 3-(3-methylbut-1-en-1-yl)-1,4-dioxo-1,4-dihydronaphthalen-2-yl acetate, have shown better antimalarial activity than lapachol itself, [10-12] showing the potential to improve upon lapachol in the search for new antimalarials.

Atovaquone (**2**) is a synthetic hydroxy-naphthoquinone, structurally related to lapachol, which is very active against *P. falciparum* in both erythrocytic and liver stages of the protozoa life cycle and was introduced in malaria therapeutics in 2000. However, resistance was observed and it is presently used in association with other antimalarial drugs [13, 14]. Atovaquone is also active against other protozoa parasites including *Toxoplasma* and *Pneumocystis.* It has been shown to

be an inhibitor of coenzyme Q and ubiquinone (**3**), which play important roles in the parasitic respiratory chain, an effect that has been related to their structural similarities. Atovaquone blocks the mitochondrial electron transport chain, specifically targeting the cytochrome bc_1 complex in the *Plasmodium* respirational system and further interfering in many processes including protein synthesis and heme biogenesis that are important for its survival [15, 16]. A similar mechanism of action could be produced by lapachol and analogues, since they also have a naphthoquinone core [17].

Recent studies suggest a "cross-relation" between the respiratory chain and pyrimidine biosynthesis [15]. Following the availability of the complete parasite genome, it was realized that *P. falciparum* is dependent on *de novo* pyrimidine biosynthesis [18]. Thus, the parasite is also susceptible to the inhibition of dihydroorotate dehydrogenase (DHODH), a flavin-dependent mitochondrial enzyme that catalyzes the fourth and rate-limiting step in the *de novo* pyrimidine biosynthetic pathway [19, 20]. Meanwhile, as demonstrated by reported X-ray co-crystal structures of human and plasmodial DHODHs bound to selective inhibitors, significant differences exist between the DHODHs from different species, in the whole sequence as well as among the amino acids forming the inhibitor binding site [18, 21, 22].

Therefore, *P. falciparum* DHODH (*Pf*DHODH) represents a target for the discovery and development of parasite-specific inhibitors that could lead to promising antimalarial lead compounds [18, 23]. Different chemical scaffolds have been identified as potent inhibitors of *Pf*DHODH that show strong selectivity for the plasmodial DHODH over that of the human host [23, 24]. A number of co-crystal structures of the human and *Pf*DHODH with bound inhibitors are available in the RCSB Protein Data Bank (www.rcsb.org), and these have provided structural insights into key protein-ligand interactions governing the selective inhibition of *Pf*DHODH [18,

21, 22]. Several computational studies have been done using various approaches with a goal of finding optimized PfDHODH inhibitors [25, 26]. In this work, we applied molecular docking to explore binding modes as well as to provide important information about the quantitative structure-activity relationship (QSAR) for the new compounds' interaction with this enzyme. Additionally, the present results might support the proposal of more potent *Pf*DHODH inhibitors [20, 27] based on the lapachol pharmacophore.

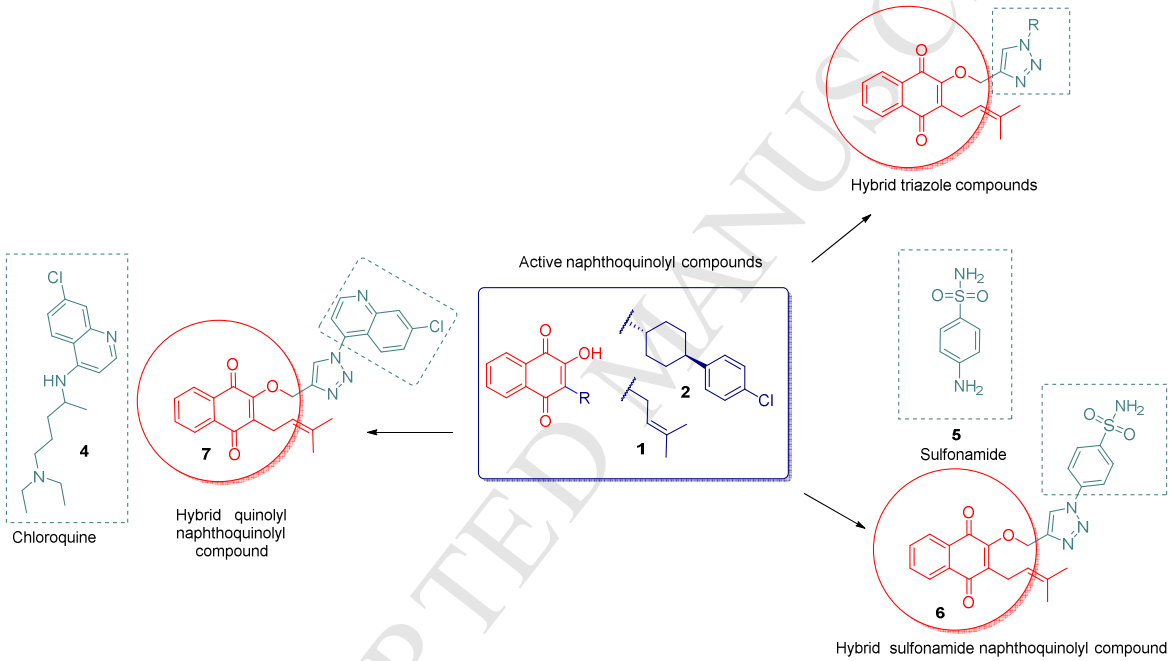

Scheme 1. *Naphthoquinonolyl-1,2,3-triazole hybrids from three different routes via click reactions.*

Recently, naphthoquinone derivatives have shown promising results as antiparasitic lead compounds [28]. Conjugated hybrid compounds could be an effective path to discovery of new drugs by associating two different pharmacophore groups with different mechanisms of action in a single molecule, [29, 30] which could yield a drug that kills the plasmodial parasites in two different ways. The chloroquine pharmacophoric group, responsible to inhibit the polymerization

of the harmful heme group into the hemozoin non toxic pigment, was also planned to be introduced in a final hybrid compound to have two possible mechanisms of action, as shown in Scheme 1 [29]. A synthetic approach to produce a hybrid molecule is via click chemistry, introduced by Sharpless, and currently widely used, [31] including for natural product activity enhancement [32-39]. Hybrid molecules can be easily produced by combining a terminal alkyne of a naphthoquinone intermediate (**6**) with different organic azides. Our strategy was to modify a known active natural product lapachol (**1**), first by alkylating at the hydroxyl position. This ether naphthoquinolyl intermediate was then reacted with different organic azides supporting sulfonamide or 7-chloroquinoline moieties besides miscellaneous aryl groups using a copper cycloaddition click reaction and to evaluate the antiplasmodial activity of the new compounds.

2. Results and discussion

Lapachol is an alkyl naphthoquinone natural product occurring in *Handronthus* species (Syn. *Tabebuia*) disclosing a large spectrum of biological activities. During the Second World War, lapachol analogues including hydrolapachol and lapidone were studied in a search for alternative antimalarial compounds. Later, a lapachol modified structure led to development of the antimalarial atovaquone, a synthetic chloride naphthoquinone [40]. Structural modification of lapachol, which is abundant in Brazilian *Handroanthus* spp. (Bignoniaceae), was the strategy aimed to prepare potentially more potent antimalarial naphthoquinones. The possibility of linking different moieties to the lapachol hydroxyl group was the inspiration for the present work, once its easy alkylation by a Williamson reaction would afford the alkynyl moiety necessary for the click reactions to be carried out. From the propargyl ether **2**, a total of 17 new naphthoquinonolyl-*1,2,3*-triazole hybrid compounds were synthesized and spectroscopically characterized.

Natural product lapachol (**1**) was isolated by basic/acid work up and further purified by silica column chromatography and the synthesized compounds were evaluated for their *in vitro* antimalarial activity against *P. falciparum* W2 that is a chloroquine resistant and mefloquine-sensitive strain. Table 1 shows the yields of the click reactions, the IC_{50} values for the *in vitro* antimalarial assay (*p*LDH method), the CC_{50} values for the cytotoxicity to HepG2 cells (MTT method) and the SI for each compound. In general, low cytotoxicity (CC_{50} > 100 µM) was observed except for the hybrid lapachol-AZT derivative (**18**) (CC_{50} < 100 µM). All the compounds disclosed IC_{50} < 100 µM and were thus more active than lapachol (IC_{50} = 123.5 ± 11.5 µM), except possibly for **21**, for which the exact IC_{50} was not determined (IC_{50} > 104.6 µM). Eleven compounds showed IC_{50} < 10 µM, with the most active being **13**, **14** and **25** with IC_{50} of 4.0 ± 1.6, 4.6 ± 1.9, and 4.1 ± 1.0 µM, respectively. The most promising compounds are **17** and **25** that disclosed the highest SI values (197.7 and 171.0, respectively). Compound **7** also has a favorable SI (128.8). Its effect might be because of a second mechanism of action, that is, the inhibition of heme polymerization, similarly to chloroquine, due to the presence of a chloroquinolyl pharmacophore group.

Table 1. Yields of click reactions affording lapachol derivatives **1**, **7**, **11**, **13**-**28**, *in vitro* antimalarial activity (IC_{50} µM) against *P. falciparum* (W2 strain), cytotoxicity (CC_{50} µM, HepG2 cells) and selectivity index (SI).

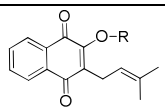

R	IC50[a] (µM)	CC_{50}[b] (µM)	SI[c]	R	IC_{50} (µM)	CC_{50} (µM)	SI

1	lapachol	123.5 ± 11.5	> 4130.7	> 33.4	**20**	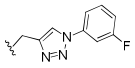	8.4 ± 4.1	264.6 ± 40.3	31.5
7	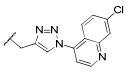	15.1 ± 3.0	1944.9 ± 55.3	128.8	**21**	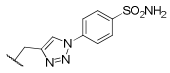	> 104.6	482.8 ± 42.7	< 4.6
11		8.2 ± 0.5	924.2 ± 65.2	112.7	**22**	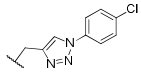	9.8 ± 3.2	1154.0± 37.8	117.7
13	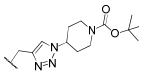	4.0 ± 1.6	136.0 ± 23.8	34.0	**23**	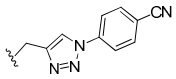	8.4 ± 1.3	707.2 ± 30.1	84.2
14	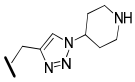	4.6 ± 1.9	570.3 ± 62.6	124.0	**24**	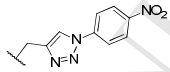	11.7 ± 0.6	539.8 ± 106.6	46.1
15	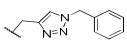	7.8 ± 1.1	413.5 ± 37.9	75.6	**25**	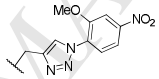	4.1 ± 1.0	701.1 ± 55.9	171.0
16	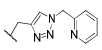	8.7 ± 3.4	657.5 ± 29.2	75.6	**26**	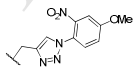	8.2 ± 5.5	531.5 ± 79.9	64.8
17	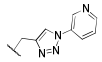	5.2 ± 1.8	1028.1± 29.2	197.7	**27**	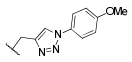	14.2 ± 1.4	200.1 ± 29.3	14.1
18	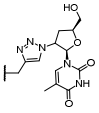	13.6 ± 3.4	60.7 ± 5.3	4.5	**28**	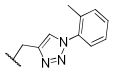	18.8 ± 3.3	256.0 ± 33.1	13.6
19	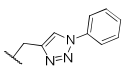	19.1 ± 1.0	100.3± 25.1	5.2					
4	Chloroquine	0.4± 0.03	393.0 ± 27.2	982.5	**2**	[d]Atovaquone	1.22 x 10^{-3} ± 0.0009	> 40.0	> 327.9

[a]IC_{50}: concentration that inhibits 50% of the parasite growth in relation to control cultures with no drugs.

[b]CC_{50}: concentration that kills 50% of HepG2 cells, 24 h after incubation with the compounds determined by the MTT method.

[c]SI: Selectivity Index = CC_{50}/ IC_{50}

Molecular modeling can provide important information about the interaction of the obtained compounds and potential parasite targets, such as DHODH. The inhibitor-binding site of *Pf*DHODH, located in proximity to the cofactor-binding site, is characterized by the presence of two regions: the H-bond pocket, comprising H185, Y528 and R265, and the hydrophobic pocket. It has been crystallographically proven that the 1,4-naphthoquinone substructure of atovaquone binds into the H-bond pocket, while its large hydrophobic substituent resides in the hydrophobic pocket. Interestingly, the compounds reported in this paper also possess a 1,4-naphthoquinone moiety, similarly to atovaquone, as well as a large hydrophobic substituent attached at position 3. On the basis of this information, molecular modeling studies were designed aiming to explore the putative binding modes of these new compounds at the inhibitor-binding site of *Pf*DHODH. In general, several available structures of the DHODH enzyme with bound inhibitors of various sizes show that there is an overlap of the portions of the structures that fit into the H-bond pocket and exhibit polar interactions with H185, Y528 and R265. On the other hand, the size of the hydrophobic pocket is variable, depending on the conformations of the side chains of F171 and F188. In addition, we observed that M536 and Y168 are two additional residues with a high degree of conformational flexibility in the same hydrophobic pocket. Therefore, in order to study the binding mode of the new ligands of variable size, we used the Induced Fit docking protocol (Schrödinger package), in which the ligand-binding site flexibility was taken into account to explain the binding modes of ligands varying in size. A summary of docking scores predicted for the interaction of the obtained compounds with *Pf*DHODH (PDB-Id: 1TV5) is given in Table 2, together with their IC_{50} values.

Table 2. *In vitro* antimalarial activity (IC_{50} in µM) and predicted docking scores (kcal/mol) of lapachol and the synthetic naphthoquinonolyl compounds with *Pf*DHODH by the Induced Fit docking protocol.

Compound	IC_{50}	Docking score	Compound	IC_{50}	Docking score
1 Lapachol	123.5 ± 11.5	-9.137	**19**	19.1 ± 1.0	-10.994
2 Atovaquone	1.22×10^{-3} ± 0.0009	-12.945	**20**	8.4 ± 4.1	-12.914
7	15.1 ± 3.0	-11.498	**21**	> 104.6	-10.12
11	8.2 ± 0.5	-9.375	**22**	9.8 ± 3.2	-12.709
13	4.0 ± 1.6	-12.504	**23**	8.4 ± 1.3	-12.608
14	4.6 ± 1.9	-12.587	**24**	11.7 ± 0.6	-12.014
15	7.8 ± 1.1	-13.449	**25**	4.1 ± 1.0	-12.96
16	8.7 ± 3.4	-13.449	**26**	8.2 ± 5.5	-12.296
17	5.2 ± 1.8	-14.55	**27**	14.2 ± 1.4	-12.08
18	13.6 ± 3.4	*	**28**	19.4 ± 3.3	-13.621

*Failed to dock into the inhibitor-binding site

The molecular docking data supported the potential interaction of lapachol and the synthetic naphthoquinonolyl compounds with the *Pf*DHODH enzyme as the putative mechanism of action and the inhibition of parasite growth *in vitro*. In general, compounds fit well into the binding pocket of *Pf*DHODH, the tightness of binding varying with the size of the ligand, which is expressed by the docking scores. In order to explain the binding of the studied compounds, the ligand-binding site is labeled as three pockets based on the binding of atovaquone: pocket 1 (P1) occupied by the 1,4-naphthoquinone moiety, pocket 2 (P2) accommodating cyclohexane, and pocket 3 (P3) occupied by the 4-chlorobenzene ring (**Figure 2**). The 1,4-naphthoquinone, a

common substructure, displayed direct interactions with R265 and Y528 in pocket P1, and its binding pose was stabilized by hydrophobic interactions with I172, I263 and V532 amino acids. The unsaturated isoprenyl moiety at position 2 of the 1,4-napthoquinone moiety occupied the proximal hydrophobic pocket P2 comprising interactions with the amino acids F188, V223, F227 and Y528. It has been shown experimentally that the side chain of F188 attains various rotameric states in P2 in order to allow the protein to accommodate ligands of variable sizes as well as to provide access to P3. Interestingly, since the binding site was kept flexible during docking studies, F188 attained a down-pointing conformation in most of the inhibitor-docked *Pf*DHODH structures, so as to accommodate the large substituents present at position 3 of 1,4-naphthoquinone. Additionally, F188 exhibited aromatic interactions with the *1,2,3*-triazole moiety in an edge-to-face manner. In addition, the *1,2,3*-triazole moiety was oriented parallel to the disulfide bridge between C175 and C184, which connects the two helices α1 and α2 of *Pf*DHODH, and exhibited hydrophobic interactions with C175, L176, C184, and other proximal amino acids. Among the studied novel molecules (**1**, **7**, **11**, **13**-**28**), major differences were observed in the relative binding of the various substituents linked to the nitrogen N1 of the *1,2,3*-triazole moiety into P3 of *Pf*DHODH. To accommodate these substituents, F171 in the α1 helix attained distinct conformations and was found to exhibit aromatic π–π stacking or other types of hydrophobic interactions. The better activity observed for compound atovaquone (**2)** over lapachol (**1)** is apparently due to the presence of the hydrophobic propargyl group which fit better into the hydrophobic pocket. The piperidine NH moiety of **14** formed H-bonds with the OH of Y168 and the backbone C=O of F171. The piperidine ring in **13** (docking score = -12.504) exhibited bidentate H-bonding with the backbone C=O of F171 and with Y168 in pocket P3. The substitution of the acetyl group for the piperidyl nitrogen (compound **19**, docking score = -

10.994) reduced the binding score, due to loss of H-bonding with F171 and Y168, which could be one of the reason behind its lesser potency against *P. falciparum*. In comparison to **24 (**docking score = -12.014), compound **25**, which contains an *o*-methoxy group in addition to a *p*-nitro, showed better binding (docking score = -12.960), due to the hydrophobic contribution in pocket P3. The sulfonamide analogue **21** displayed poorer binding affinity (docking score = -10.120), which agreed with its experimentally-demonstrated lower activity (IC_{50}). The docking study suggested **17** as the compound with the highest affinity for *Pf*DHODH. As shown in **Figure 2**, the 3-pyridyl substituent (**17**) exhibited aromatic π–π stacking interactions with F171 (in the α1-helix) as well as H-bonding with the backbone NH of M536 along with hydrophobic interactions. In addition, it favored the CH – π interaction between the *1,2,3*-triazole and F188 (**Figure 2**). Attempts of docking with **18** failed, probably because of its overall large size. Possibly the pocket P3 failed to accommodate the bulky substituent on N1 of its *1,2,3*-triazole core. Therefore, compound **18** is predicted not to act through the inhibition of *Pf*DHODH enzyme for its antimalarial activity (IC_{50} = 13.6 ± 3.4 µM). The quinoline analogue **7** also displayed comparatively poorer binding affinity that was apparently due to the bulkiness of its quinoline ring, leading to impaired interaction in pocket P3. Overall, the docking study suggested compound **17** as the lead against *Pf*DHODH (score = -14.550) (IC50 = 5.2 ± 1.8 µM; SI = 197.7). The structure-activity relationships could be further explored by incorporating small substitutions on the 3-pyridyl ring. Such structural modifications are expected to enhance enzyme binding affinity and thus lead to compounds with higher potency against the parasite.

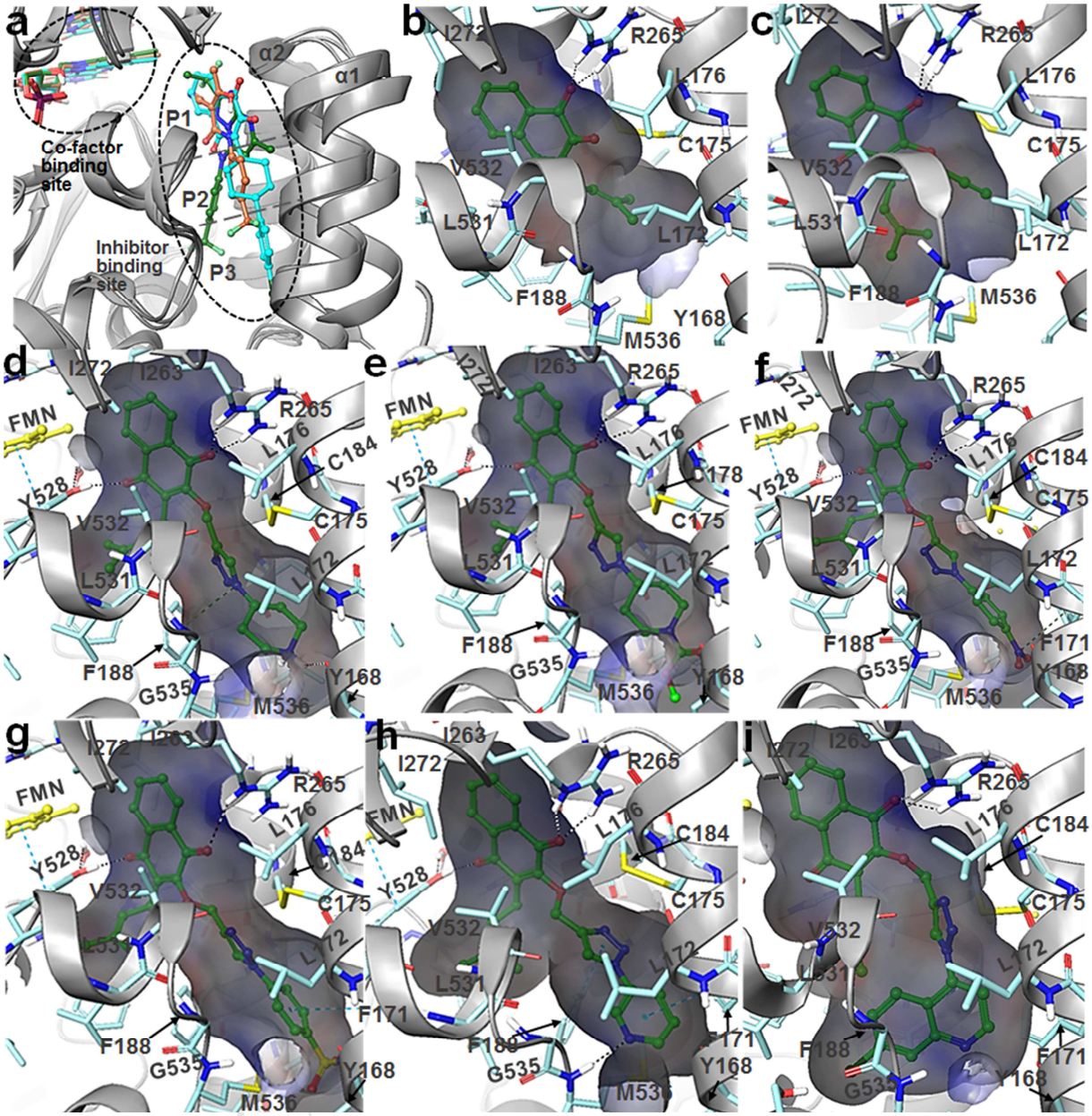

Figure 2. (a) Superposed view of the X-ray structure of rat DHODH with bound atovaquone (cyan carbon) (PDB-ID: 1UUM) and two structures of *Pf*DHODH with bound DSM267 (dark green carbon) (PDB-ID: 3SFK) and A26 (orange carbon) (PDB-ID: 1TV5). The inhibitor and proximal co-factor binding sites are encircled with black dashed lines. The inhibitor binding site is categorized into three sub-pockets as Pocket 1 (P1), Pocket 2 (P2) and Pocket 3 (P3) (roughly

separated by gray long-dashed lines). **(b-i)** Depiction of predicted binding modes of (b) **1**, (c) **11**, d) **14**, (e) **13**, (f) **24**, (g) **21**, (h) **17**, and (i) **7**, all with *Pf*DHODH (1TV5). The protein is shown as gray-colored cartoon, while ligands are shown as ball-and-stick form. The inhibitor binding sites in images b-i are depicted as surface view, colored according to the electrostatic potential (blue: electropositive, red: electronegative). Some π-π interactions are shown with blue dashed lines and some hydrogen bonds or other electrostatic interactions are shown with black dotted lines.

3. Conclusion

The present work describes the synthesis of 18 naphthoquinonolyl-*1*,*2*,*3*-triazole compounds based on natural product modification with antiplasmodial activity. Lapachol derivatives disclosed higher activity than the natural product. Six of these final modified lapachol *1*,*2*,*3*-triazole compounds showed SI > 100. The most promising compounds such as compounds **17**, **22** and **25** have some structural similarities such as a substituted aryl side chain in the triazole ring. The triazole naphthoquinolyl compounds with only phenyl (compound **19** with **SI** = 5.3) or benzyl (compound **15** with **SI** = 53.0) moieties had moderate activity. However, the presence of heteroatoms such as a chlorine substituent or a nitrogen on the aromatic ring played an important role (**SI** = 51.0, 75.6, 128.8 and 197.7 for compounds **22**, **16**, **7** and **17**, respectively). Other promising compounds such as **25** (**SI** of 171.0**)** demonstrate that nitro and methoxy groups also can play an important role, depending upon their site of attachment. Atovaquone and compound **11** with terminal alkyne and pyrimidine moieties, with **SI** of 112.7 and 124.0, respectively, also provide important information for future studies. Docking studies support the possibility that these compounds do target *Pf*DHODH. Based on the best docking scores, **16** was identified as the best lead compound against *Pf*DHODH. Structure-activity relationship studies could further

be explored by incorporating small substitutions on the 3-pyridyl ring of **17**. Doing so is expected to enhance enzyme binding affinity and thus lead to compounds with higher potency against the *Pf* parasite.

4. Materials and Methods

4.1. Biological activity

4.1.1. Continuous cultures of *Plasmodium falciparum*

P. falciparum W2 clone, which is chloroquine-resistant and mefloquine-sensitive [41], was kept in a continuous culture at 37 °C in human erythrocytes using the candle jar method [41, 42]. The antimalarial effect of the compounds was measured by the pLDH assay [43, 44]. Parasites were kept in complete culture medium (RPMI) containing sodium bicarbonate (21 mM), D-glucose (11 mM), HEPES (25 mM), hypoxanthine (300 µM) and gentamicin (40 µg/ml) that was supplemented with 10% human plasma on culture dishes, the culture medium being changed daily. All experiments were performed in triplicate. The compounds were tested in triplicate at each concentration. The cultures with predominantly ring-stage parasites were concentrated by sorbitol-synchronization [45]. A suspension of red blood cells with 0.05% parasitemia and 1.5% hematocrit was distributed in a 96-well micro titer plate (180 µl/well). The parasite growth was evaluated by the pLDH assay, as summarized below.

4.1.2. Evaluation of the *in vitro* antimalarial activity by the *p*LDH assay

The antimalarial effects of the compounds and of the controls were measured by the lactate dehydrogenase of *Plasmodium falciparum* (pLDH) assay as previously described [20], with

minor modifications. Briefly, ring-stage parasites in sorbitol-synchronized blood cultures were added to 96-well culture plates at 2% parasitemia and 1% hematocrit and then incubated with the test drugs that were diluted in complete medium, from 50 mg mL^{-1} stock solutions in DMSO, at a final concentration of 0.002% (v/v) and stored at –20 ºC. After a 48 h incubation period, the plates were frozen (–20 ºC for 24 h) and thawed for the pLDH assay. The hemolyzed cultures were transferred to another 96-well culture plate, and Malstat® and nitro blue tetrazolium salt and phenazine ethosulphate (NBT/PES) reagents were added. After 1 h of incubation at 37 ºC in the dark, the absorbance was read at 570 nm in a spectrophotometer (Infinite®200 PRO, Tecan). The results were evaluated with the software Microcal Origin 8.5 for determination of the dose-response curves plotted with sigmoidal fit [46]. The IC_{50} was determined by comparison with controls with standard drug and without drugs.

4.1.3. Cytotoxicity evaluation in human hepatoma cell cultures – HepG2 cell

Hepatoma cells HepG2 cell were maintained at 37 ºC in 5% CO_2 in 75 cm^2 sterile culture flasks (Corning®) with RPMI 1640 culture medium supplemented with 5% FBS, penicillin (10 U/ml), and streptomycin (100 g/ml), with changes of medium twice a week. The cells were maintained in weekly passages (at 1:3 dilutions in sterile culture flasks) and grown to 80% [47]. They were used for experiments after being trypsinized (0.05% trypsin/0.5 mM EDTA) and plated on 96 well microplates [48]. The test samples and controls (chloroquine and atovaquone) were diluted to a final concentration of 0.02% DMSO in culture medium to yield four concentrations in serial dilutions starting at 1,000 mg/ml. After 24 h incubation at 37 °C, 18 µl of MTT solution (5 mg/ml in PBS) were added to each well, followed by another 90 min incubation at 37 °C. The supernatant was then removed, and 180 µl of DMSO was added to each well. The culture plates were read in a spectrophotometer with a 570 nm filter [47]. The minimum cytotoxicity

concentration was determined as described previously, with slight modifications (DMSO was used instead of ethanol for solubilizations and the positive control used was chloroquine instead of primaquine). Each test was performed in duplicate, and the concentration that killed 50% of the cells (CC_{50}) was determined [49]. The selectivity index (SI) for the antimalarial activity was then calculated based on the ratio between CC_{50} and IC_{50} for the *in vitro* activity against *P. falciparum* as described [50]. Most of the compounds showed SI > 10 and could be considered non-toxic [51].

4.2. Extraction

4.2.1. Plant material

Trunkwood of *Handroanthus serratifolius* (Vahl) S.O. Grose were collected from specimens identified by Dr. Prof. João Renato Stehmann, Instituto de Ciências Biológicas, Universidade Federal de Minas Gerais. A voucher specimen (BHCB 32995) is deposited in the herbarium of Instituto de Ciências Biológicas da Universidade Federal de Minas Gerais, Belo Horizonte, MG, Brazil.

4.2.2. Extraction and isolation of lapachol

The pulverized wood material (3000 g) was macerated with 10 L of a 2.5% sodium carbonate solution for 12 h. The suspension was filtered and the filtrate was acidified with $HCl_{(aq)}$ conc., resulting in precipitation of a dark viscous material (180.0 g) that was filtered under vacuum, dried in an oven at 45 ºC and further extracted with dichloromethane in a Soxhlet apparatus for 12 h. Further purification was performed by chromatography through a silica gel column. The product was eluted with dichloromethane/hexane (1:1 v/v) as a bright yellow solid (5.3 g) and was characterized as lapachol (**1**) by classic methods including ^{1}H NMR and ^{13}C NMR.

4.3. Chemistry

4.3.1. General

Chemicals and reagents were purchased from commercial suppliers and used as received unless noted otherwise. Reactions were monitored by thin layer chromatography (TLC) on precoated 0.2 mm silica gel 60 F_{254} (Merck) plates and visualized in several ways with an ultraviolet light source at 254 nm, by spraying with Hanissam reagent (Ceric ammonium molibidate-CAM), anisaldehyde sulfuric acid, Dragendorff reagent or iodine. All reactions were performed in standard dry glassware without inert atmosphere. Evaporation and concentration were done in standard rotavapors (Büchi and IKA) under vacuum. TLC was carried out with silica gel 60 with fluorescent indicator (e.g., Silica Gel F-254 or IB-F, Merck) after previous activation with heating at 100 °C overnight and visualization by UV light or Dragendorff reagent. Melting points (mps) were measured in a Fisher-Jones melting point apparatus and are uncorrected. ^{1}H and ^{13}C NMR spectra were measured on a Bruker Advance DPX 200, Fourier 300HD and DRX400 with FT analysis. Chemical shifts are reported δ (ppm) with $SiMe_4$ as internal standard. Coupling constants (*J*) are given in Hertz. The deuterated solvents used were CD_3OD, $CDCl_3$ or DMSO-d_6. All 2D NMR data were recorded at 400 MHz (Bruker DRX400), heteronuclear single quantum coherence (HSQC) using *J* 145 Hz, and heteronuclear multiple-bond correlation (HMBC) using *J* 8 Hz. Infrared spectra were recorded on a FT-IR, Spectrum One (Perkin-Elmer) with ATR system and are reported in wave numbers (cm^{-1}). Samples were diluted with methanol-formic acid 0.1% solution. High resolution mass spectrometry (HRMS) data were recorded on a Shimadzu liquid chromatography-mass spectrometry ion trap and time-of-flight (LCMS-IT-TOF) spectrometer using electrospray ionization (ESI) and Waters ACQUITY® tandem quadrupole detector (TQD).

4.3.2. Materials

4,7-Dichloroquinoline, benzyl bromide, aniline, 3-(bromomethyl)pyridine, 3-(bromomethyl)pyridine hydrobromide, 2-bromopyridine, 2-azidotolueno solution, sulfonamide, 2-methoxy-4-nitroaniline, 4-fluoroaniline, 4-methoxy-2-nitroaniline, 4-aminobenzonitrile, 4-hydroxypiperidine, 1-Boc-4-hydroxypiperidine, molecular sieves A4, molecular sieves A3, triethylamine, 3-bromoprop-1-yne, Ziduvudine, Hydrogen Chloride 1M solution, RPMI 1640 medium, sodium bicarbonate, D-glucose, HEPES, hypoxanthine, gentamicin, D-sorbitol, PBS, BSA, TMB, FBS, penicillin, streptomycin, tripsin/EDTA, and DMSO were obtained from Sigma-Aldrich® USA, Ltd. Copper sulphate pentahydrate was obtained from Reagen®, ascorbic acid was obtained from Synth®, MPFG-55P and MPFM-55A antibodies were purchased from ICLLABS®, sulfuric acid, diethyl ether, dichloromethane, hexane, ethyl acetate, chloroform, sodium bicarbonate and sodium sulphate were obtained from FMaia®, and were used without further purification. Glassware was from Hialoquímica, Ltd.

4.3.3 Synthetic Approach

Lapachol (**1**) was O-alkylated using propargyl bromide propyne in acetone, providing the alkyne naphthoquinonolyl intermediate (**11**) in good yield, after optimizing conditions to provide this regioisomer rather than **12**. Using parallel synthesis, 4,7-dichloroquinoline (**8**) was functionalized in sodium azide, via a nucleophilic substitution reaction (S_NAR), to provide compound **9** [52]. Next, these two intermediates were combined by Copper-Catalyzed-Azide-Alkyne Cycloaddition (CuAAC) to produce the lapachol-*1*,*2*,*3*-triazole hybrid **7** as shown in **Scheme 2**.

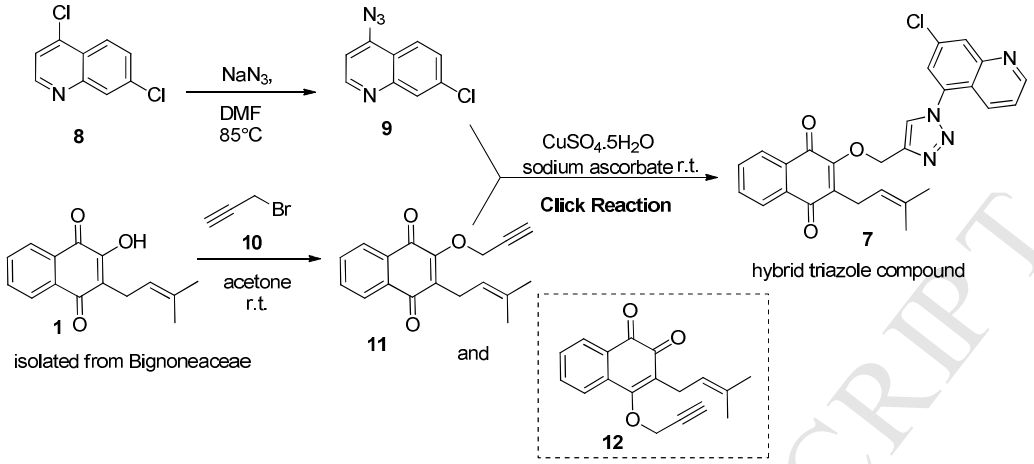

Scheme 2. *Synthesis of the naphthoquinonolyl hybrid **7** containing a 7-chloroquinoline moiety obtained via click reaction between the terminal alkyne **11** and the organic azide **9** in a convergent route.*

Different azides could also by prepared by bimolecular nucleophilic substitution (S_N2) or aromatic nucleophilic substitution (S_NAr) as shown in **Scheme 3** [53]. Commercially available alkyl and aryl halides and Zidovudine® (AZT) were used as shown in **Scheme 3**. Compounds **13**-**17** were prepared in high yield reactions (60 to 95%). Compound **14** was obtained after Boc deprotection of **13** using anhydrous acid conditions.

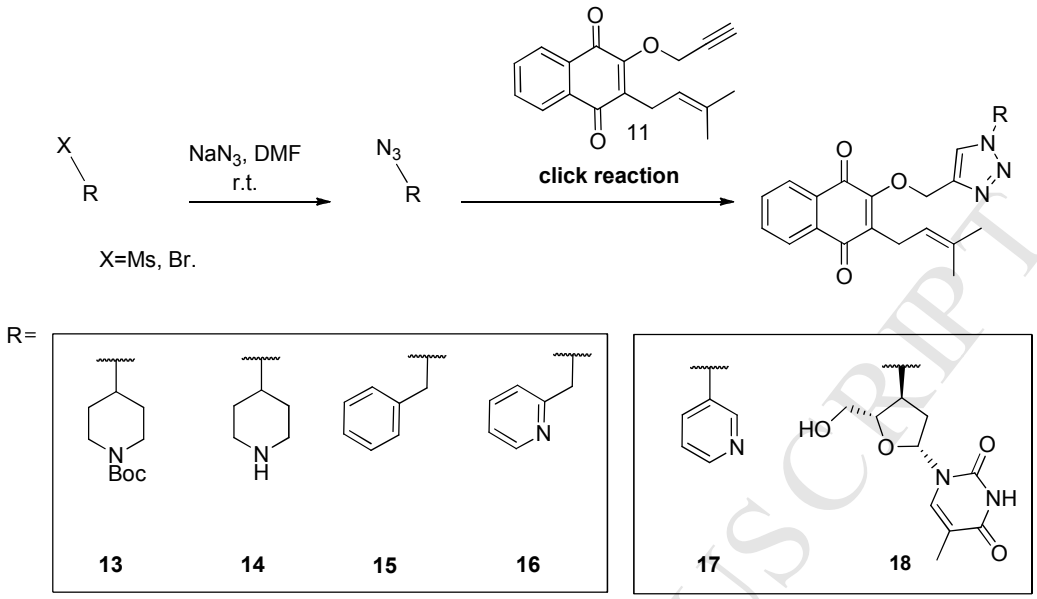

Scheme 3. *Naphthoquinonolyl hybrid synthetic route for click reactions between* ***11*** *and organic azides* ***13-18****.*

Another explored route to azides was provided by aromatic nucleophilic substitution (S_NAr) via diazotization reaction of commercially available anilines (**Scheme 4**).

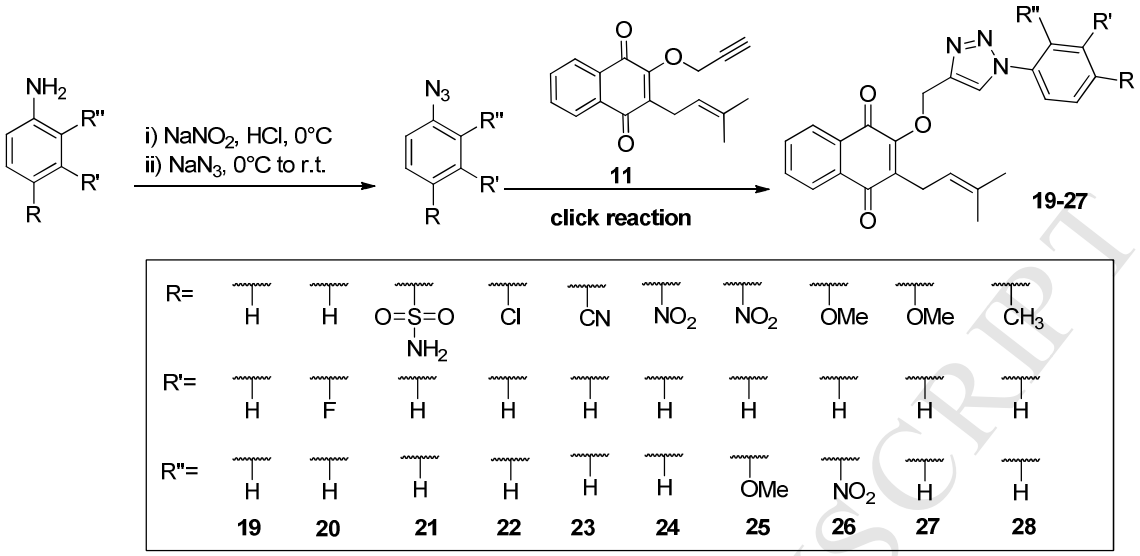

Scheme 4. *Aromatic nucleophilic substitution (S_NAr) forming diazonium salts "in situ" providing different organic azides as starting materials for click reactions with alkyne* ***11***.

The structures of the products were characterized by spectroscopic data including HRMS-ESI-IT-TOF, IR, ^{1}H and ^{13}C NMR (Cf. Supporting Information).

4.3.4. Isolation, Synthesis and characterization

Lapachol

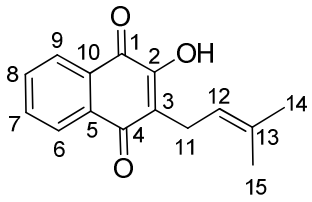

Yield: 0.5% from bark, orange solid, IR (λ_{max}, cm^{-1}): 3348, 2972, 2907, 1659, 1638, 1591, 1456, 1367, 1351, 1336, 1237, 1209, 1182, 1153, 1046, 1028, 936, 846, 675. ^{1}H NMR (200 MHz, $CDCl_3$): δ 8.13-8.05 (m, 2H, H_7 and H_8), 7.78-7.63 (m, 2H, H_6 and H_9), 7.34 (s, 1H, O<u>H</u>), 5.21 (m, 1H, H_{12}), 3.30 (s, 3H, J = 6.6 Hz, H_{11}), 1.79 (s, 3H, H_{14}), 1.68 (s, 3H, H_{15}). ^{13}C NMR (50 MHz, $CDCl_3$): δ 184.46, 181.71, 152.72, 134.77, 133.73, 133.04, 132.78, 129.54, 126.78,

126.02, 123.57, 119.73, 25.67, 22.65, 17.85. HRMS-ESI-IT-TOF: m/z calculated $C_{15}H_{15}O_3$ (M+H) 243.1021, found 243.1152.

Azides

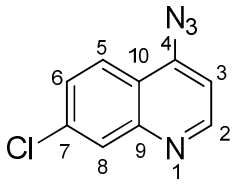

4-Azido-7-chloro-quinoline (**9**) [54]

To a solution of 4,7-dichloroquinoline (**8**) (2.0 g, 10 mmol) in 5 mL anhydrous DMF and molecular sieves A4, sodium azide (1.3 g, 20 mmol) was added in one portion at room temperature, and the resulting mixture stirred at 85 ^{o}C for 8 h, when TLC indicated reaction completion. The reaction mixture was allowed to cool to room temperature and then it was diluted with 100 mL CH_2Cl_2, washed with water (3 x 40 mL), dried over anhydrous Na_2SO_4, and evaporated to dryness. The resulting product residue was purified by small column chromatography eluted with CH_2Cl_2/Hexane mixture 1:1 to yield the final pure product as colorless, needle-like crystals (1.8 g, 91%), mp 115 °C (from CH_2Cl_2/Hex), Rf (EtOAc/Hex 3:7) 0.29.

IR (λ_{max}, cm^{-1}): 3079, 3036, 2983, 2118, 1670, 1608, 1578, 1564, 1557, 1489, 1440, 1417, 1373, 1351, 1300, 1278, 1199, 1146, 1090, 1071, 1011, 963, 896, 880, 840, 818, 777, 768, 671, 663. ^{1}H NMR (200 MHz, $CDCl_3$): δ 8.76 (1H, d, J = 5.0 Hz, H_2), 8.00 (1H, d, J = 2.0 Hz, H_8), 7.88 (1H, d, J = 8.8 Hz, H_5), 7.49 (1H, dd, J = 2.0 Hz, J = 8.8 Hz, H_6) 7.13 (1H, d, J = 5.0 Hz, H_3). ^{13}C NMR (50 MHz, $CDCl_3$): δ 151.33, 149.59, 146.30, 136.57, 128.23, 127.52, 123.77, 119.91, 108.73.

General methodology to produce azides by nucleophilic aromatic substitution

Sodium azide (1.5 equivalent) (**9**) and a commercially-available alkyl halide (1.0 equivalent) were mixed in anhydrous DMF (2 mL) and stirred at room temperature. The reaction was left running overnight and was stopped when it was completed as shown by TLC. Work-up of the

reaction mixture with CH_2Cl_2, brine and water (2 x 10 mL), was followed by drying over Na_2SO_4 and the product was used without further purification by column chromatography.

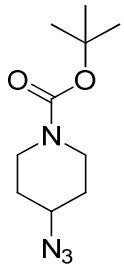

Tert-butyl 4-azidopiperidine-1-carboxylate (**30**).

IR (λ_{max}, cm^{-1}): 2976, 2932, 2863, 2090, 1687, 1468, 1451, 1416, 1392, 1364, 1129, 1087, 1019, 938, 863, 816, 769, 725. ^1H NMR (200 MHz, $CDCl_3$): δ 4.82 (m, 1H, H_4), 3.73-3.20 (m, 4H, H_2), 3.00 (s, 3H, H_5), 1.99-1.81 (m, 5H, H_3 and H_4), 1.42 (s, 9H, H_7). ^{13}C NMR (50 MHz, $CDCl_3$): δ 154.40, 79.86, 40.45, 38.76, 31.59, 28.29, 8.55.

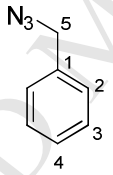

(Azidomethyl)benzene (**31**).

Yield: 98%, viscous colorless oil, IR (λ_{max}, cm^{-1}): 3127, 3047, 2924, 2849, 1610, 1593, 1560, 1504, 1449, 1438, 1348, 1310, 1244, 1115, 1046, 1018, 922, 875, 834, 822, 813, 767, 672. ^1H NMR (200 MHz, $CDCl_3$): δ 7.49-7.44 (m, 5H), 4.39 (M, 2H). ^{13}C NMR (50 MHz, $CDCl_3$): δ 135.38, 128.73, 128.50, 128.14, 128.13, 54.60 HRMS-ESI-IT-TOF: m/z calculated $C_7H_8N_3$ (M+H) 134.0718, found 134.0758.

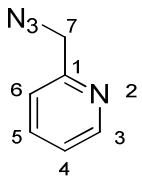

2-(Azidomethyl)pyridine (**32**).

IR (λ_{max}, cm^{-1}): 3034, 2089, 1571, 1508, 1474, 1420, 1285, 1237, 1189, 1140, 1124, 1100, 1038, 1019, 978, 935, 909, 857, 797, 700, 687. ^{1}H NMR (200 MHz, $CDCl_3$): δ 8.60 (d, 1H, J = 4.2 Hz), 7.73 (t, 1H, J = 7.6 Hz), 7.34 (d, 1H, J = 7.6 Hz), 7.30 (t, 1H, J = 4.2 Hz), 4.39 (M, 2H). ^{13}C NMR (50 MHz, $CDCl_3$): δ 155.57, 149.55, 136.99, 122.91, 121.99, 53.49. HRMS-ESI-IT-TOF: m/z calculated $C_6H_7N_4$ (M+H) 135.0671, found 135.0744.

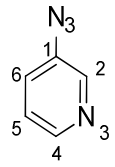

3-Azidopyridine (**33**).

IR (λ_{max}, cm^{-1}): 3064, 3036, 2090, 1593, 1491, 1470, 1454, 1341, 1293, 1278, 1174, 1128, 1075, 1025, 1002, 895, 810, 745, 685. ^{1}H NMR (200 MHz, $CDCl_3$): δ 8.02 (m, 2H), 6.97-6.93 (m, 2H). ^{13}C NMR (50 MHz, $CDCl_3$): δ 145.34, 140.63, 136.36, 125.16, 123.45, HRMS-ESI-IT-TOF: m/z calculated $C_5H_5N_4$ (M+H) 121.0514, found 121.0596.

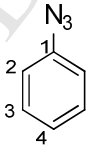

Azidobenzene (**34**).

IR (λ_{max}, cm^{-1}): 3247, 3064, 3036, 2122, 2090, 1593, 1490, 1471, 1454, 1293, 1279, 1173, 1128, 1075, 895, 820, 810, 685.^{1}H NMR (200 MHz, $CDCl_3$): δ 7.32 (t, 2H, J = 7.6 Hz, H_3), 7.11 (t, 1H, J = 7.6 Hz, H_4), 7.00 (d, 2H, J = 7.6 Hz, H_2). ^{13}C NMR (50 MHz, $CDCl_3$): δ 139.96, 129.65, 124.77, 118.94.

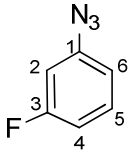

1-Azido-3-fluorobenzene (**35**).

IR (λ_{max}, cm^{-1}): 3075, 2107, 1589, 1484, 1446, 1446, 1294, 1207, 1162, 1153, 1108, 1099, 944, 922, 858, 843, 767, 673, 660. ^{1}H NMR (200 MHz, $CDCl_3$): δ 7.23 (t, 1H, J = 6.8 Hz, H_5), 6.83-6.66 (m, 3H, H_2, H_4 and H_6). ^{13}C NMR (50 MHz, $CDCl_3$): δ 164.89, 160.97, 141.97, 141.77, 130.82, 130.63, 114.58, 111.92, 111.49, 106.79, 106.30.

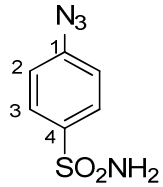

Azido-benzenesulfonamide (**36**).

IR (λ_{max}, cm^{-1}): 3398, 3076, 2102, 1638, 1510, 1488, 1464, 1260, 1017, 951, 916, 849, 806, 822, 813, 764, 703. ^{1}H NMR (200 MHz, DMSO-d_6): δ 7.84 (d, 2H, J = 7.0 Hz, H_3), 7.37 (sl, 2H, $N\underline{H_2}$), 7.28 (d, 2H, J = 7.0 Hz, H_2). ^{13}C NMR (50 MHz, DMSO-d_6): δ 142.88, 140.45, 127.58, 119.40. HRMS-ESI-IT-TOF: m/z calculated $C_6H_6N_4O_2SNa$ (M+Na) 221.0109, found 221.0100.

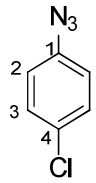

1-azido-4-chlorobenzene (**37**).

IR (λ_{max}, cm^{-1}): 2924, 2849, 2120, 2089, 1592, 1484, 1292, 1269, 1174, 1128, 1090, 1011, 821, 744, 707. ^{1}H NMR (200 MHz, $CDCl_3$): δ 7.25 (d, 2H, J = 8.6 Hz, H_3), 6.88 (d, 2H, J = 8.6 Hz, H_2). ^{13}C NMR (50 MHz, $CDCl_3$): δ 138.53, 130.08, 129.66, 120.09.

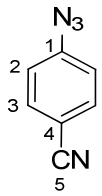

4-Azidobenzonitrile (**38**).

IR (λ_{max}, cm^{-1}): 3400, 3222, 3094, 3043, 2974, 2142, 2105, 1703, 1658, 1598, 1503, 1448, 1416, 1377, 1303, 1278, 1176, 1126, 1110, 965, 942, 919, 818, 747, 704. ^{1}H NMR (200 MHz, $CDCl_3$): δ 7.64 (d, 2H, J = 8.8 Hz, H_3), 7.11 (d, 2H, J = 8.8 Hz, H_2). ^{13}C NMR (50 MHz, $CDCl_3$): δ 144.85, 133.71, 129.88, 128.15, 119.65, 118.17, 108.32. HRMS-ESI-IT-TOF: m/z calculated $C_7H_4N_4Na$ (M+Na) 167.0334, found 167.0898.

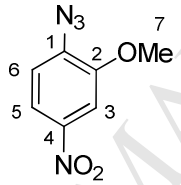

1-Azido-2-methoxy-4-nitrobenzene (**39**).

Yield: 80%, orange solid, IR (λ_{max}, cm^{-1}): 3116, 3086, 2924, 2849, 2112, 1607, 1588, 1509, 1498, 1441, 1418, 1340, 1311, 1264, 1250, 1186, 1135, 1075, 1009, 916, 903, 818, 812, 743, 715, 698. ^{1}H NMR (200 MHz, $CDCl_3$): δ 7.45 (d, 1H, J = 4.8 Hz, H_5), 7.23 (s, 1H, H_3), 7.20 (d, 1H, J = 5.4 Hz, H_6), 3.86 (s, 3H, H_7). ^{13}C NMR (50 MHz, $CDCl_3$): δ 156.55, 141.25, 127.09, 121.99, 120.97, 110.22, 56.06. HRMS-ESI-IT-TOF: m/z calculated $C_7H_6N_4O_3Na$ (M+Na) 217.0338, found 217.0248.

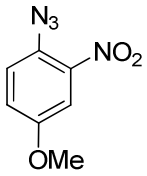

1-Azido-4-methoxy-2-nitrobenzene (**40**).

IR (λ_{max}, cm^{-1}): 3116, 3086, 2924, 2849, 2112, 1607, 1588, 1509, 1498, 1441, 1418, 1340, 1311, 1264, 1250, 1186, 1135, 1075, 1009, 916, 903, 818, 812, 743, 715, 698. ^{1}H NMR (200 MHz, $CDCl_3$): δ 7.45 (d, 1H, J = 4.8 Hz, H_5), 7.23 (s, 1H, H_3), 7.20 (d, 1H, J = 5.4 Hz, H_6), 3.86 (s, 3H, H_7). ^{13}C NMR (50 MHz, $CDCl_3$): δ 156.55, 141.25, 127.09, 121.99, 120.97, 110.22, 56.06. HRMS-ESI-IT-TOF: m/z calculated $C_7H_6N_4O_3Na$ (M+Na) 217.0338, found 217.0248.

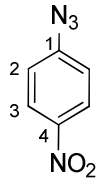

1-Azido-4-nitrobenzene (**41**).

IR (λ_{max}, cm^{-1}): 3225, 3003, 2954, 2910, 2836, 2099, 1712, 1501, 1284, 1240, 1180, 1172, 1108, 1031, 822, 754. ^{1}H NMR (200 MHz, $CDCl_3$): δ 8.23 (d, 2H, J = 9.0 Hz, H_3), 7.13 (d, 2H, J = 9.0 Hz, H_2). ^{13}C NMR (50 MHz, $CDCl_3$): δ 146.81, 144.64, 125.50, 119.33.

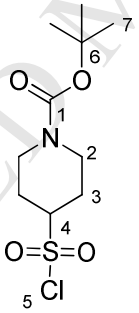

Tert-butyl 4-(methylsulfonyl)piperidine-1-carboxylate (**13**).

^{1}H NMR (200 MHz, $CDCl_3$): δ 4.82 (m, 1H, H_4), 3.73-3.20 (m, 4H, H_2), 3.00 (s, 3H, H_5), 1.99-1.81 (m, 5H, H_3 and H_4), 1.42 (s, 9H, H_7). ^{13}C NMR (50 MHz, $CDCl_3$): δ 154.40, 79.86, 40.45, 38.76, 31.59, 28.29, 8.55. HRMS-ESI-IT-TOF: m/z calculated $C_{11}H_{22}NO_4S$ (M+H) 264.1270, found 264.1242.

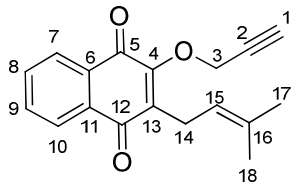

2-(3-Methylbut-2-enyl)-3-(prop-2-ynyloxy)naphthalene-1,4-dione (**1**)

Lapachol was dissolved in anhydrous acetone, K_2CO_3 was added and the mixture was stirred for 5 minutes. Then a solution of bromo-propine was added slowly in drops at r.t. and left stirred for 72 hours at 35 °C. The reaction was completed by TLC, concentrated, elaborated with ethyl acetate and water, dried over Na_2SO_4 and purified by Prep-TLC using DCM/Hexane 1:1 as eluent to yield a yellow solid as major product.

Yield: 35%, mp 135-137 ºC, IR (λ_{max}, cm^{-1}): 3117, 3074, 3033, 2924, 2883, 1664, 1651, 1609, 1592, 1578, 1497, 1455, 1336, 1300, 1261, 1238, 1193, 1166, 1052, 948, 929, 849, 818, 795, 768, 700. ^{1}H NMR (200 MHz, $CDCl_3$): δ 7.95-7.88 (m, 2H, H_8 and H_9), 7.60-7.56 (m, 2H, H_7 and H_{10}), 5.07-5.06 (m, 3H, H_3 and H_{15}), 3.26 (d, 2H, J = 7.4 Hz, H_{14}), 2.55 (t, 1H, J = 7.4 Hz, H_1), 1.72 (s, 3H, H_{18}), 1.60 (s, 3H, H_{17}). ^{13}C NMR (50 MHz, $CDCl_3$): δ 184.72, 181.34, 154.76, 136.31, 133.62, 133.57, 133.10, 131.76, 131.09, 126.07, 125.93, 119.76, 78.37, 25.65, 25.60. HRMS-ESI-IT-TOF: m/z calculated $C_{18}H_{17}O_3$ (M+H) 281.1178, found 281.0938.

General methodology for click reactions: 4-Azido-compound and lapachol alkyne were dissolved in CH_2Cl_2 (2 mL), followed by addition of $CuSO_4.5H_2O$ (0.3 equivalents) and an aqueous solution of sodium ascorbate (0.6 equivalents) (2 mL) freshly prepared. The reaction mixture was left overnight and the reaction was stopped when it was completed as shown by TLC. Work-up of the reaction mixture was done with CH_2Cl_2 and water (3 x 10 mL), dried over Na_2SO_4 and finally purified by preparative TLC or column chromatography with DCM/Hexane (1:1 v/v).

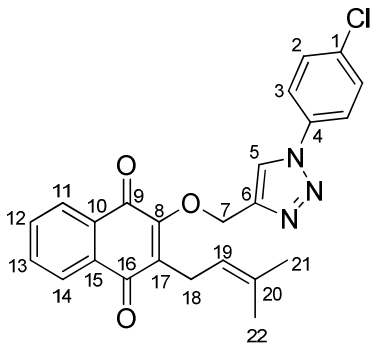

2-((1-(4-Chlorophenyl)-1H-*1,2,3*-triazol-4-yl)methoxy)-3-(3-methylbut-2-enyl)naphthalene-1,4-dione

Yield: 69%, mp 151-155 ºC, IR (λ_{max}, cm^{-1}): 3087, 2909, 1657, 1610, 1593, 1502, 1440, 1422, 1349, 1331, 1306, 1259, 1239, 1211, 1191, 1092, 1048, 950, 932, 844, 722. ^{1}H NMR (400 MHz, $CDCl_3$): δ 8.17 (s, 1H, H_5), 8.10-8.05 (m, 2H, H_{12} and H_{13}), 7.72-7.69 (m, 4H, H_3, H_{11} and H_{14}), 7.51 (d, 2H, J = 8.6 Hz, H_2), 5.60 (m, 1H, H_7), 5.04 (t, 1H, J = 7.2 Hz, H_{19}), 3.28 (d, 2H, J = 7.2 Hz, H_{18}), 1.72 (s, 3H, H_{22}), 1.63 (s, 3H, H_{21}). ^{13}C NMR (100 MHz, $CDCl_3$): δ 185.02, 181.90, 155.99, 144.99, 135.90, 135.52, 134.77, 133.88, 133.83, 133.27, 132.15, 131.51, 129.98, 126.36, 126.14, 121.76, 121.45, 119.83, 66.12, 25.68, 23.30, 17.93. HRMS-ESI-IT-TOF: m/z calculated $C_{24}H_{20}ClN_3O_3$ (M+Na) 456.1091, found 456.1164.

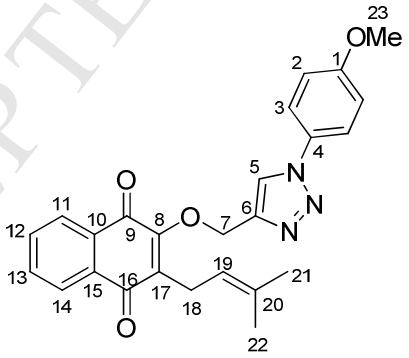

2-((1-(4-Methoxyphenyl)-1H-*1,2,3*-triazol-4-yl)methoxy)-3-(3-methylbut-2-enyl)naphthalene-1,4-dione

Yield: 71%, mp 116-125 ºC, IR (λ_{max}, cm^{-1}): 3022, 3008, 2921, 1662, 1610, 1592, 1541, 1517, 1439, 1332, 1303, 1241, 1191, 1045, 951, 830, 809, 700, 666.^{1}H NMR (200 MHz, $CDCl_3$): δ 8.12 (s, 1H, H_5), 8.06-8.04 (m, 2H, H_{12} and H_{13}), 7.71-7.67 (m, 2H, H_{11} and H_{14}),7.63 (d, 2H, J =

8.8 Hz, H_3), 7.02 (d, 2H, *J* = 8.8 Hz, H_2), 5.60 (s, 1H, H_7), 5.03 (t, 1H, *J* = 7.2 Hz, H_{19}), 3.86 (s, 3H, H_{23}), 3.26 (d, 2H, *J* = 7.2 Hz, H_{18}), 1.72 (s, 3H, H_{22}), 1.63 (s, 3H, H_{21}). ^{13}C NMR (50 MHz, $CDCl_3$): δ 185.27, 182.03, 160.05, 156.16, 135.37, 144.51, 135.91, 134.03, 133.96, 133.45, 132.15, 131.55, 130.48, 126.49, 126.29, 122.34, 121.94, 119.93, 114.93, 66.30, 55.76, 25.89, 23.40, 18.08. HRMS-ESI-IT-TOF: m/z calculated $C_{25}H_{23}N_3O_4$ (M+Na) 452.1586, found 452.1485.

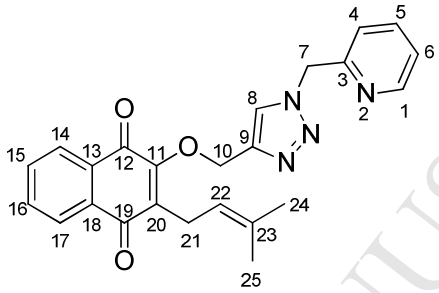

2-(3-Methylbut-2-en-1-yl)-3-((1-(pyridin-2-ylmethyl)-1H-*1,2,3*-triazol-4-yl)methoxy)naphthalene-1,4-dione

Yield: 43%, mp 82-88 ºC, IR (λ_{max}, cm^{-1}): 3131, 2923, 1651, 1607, 1591, 1476, 1456, 1437, 1372, 1330, 1307, 1264, 1244, 1192, 1154, 1126, 1053, 952, 921, 845, 827, 767, 747, 706. ^{1}H NMR (200 MHz, $CDCl_3$): δ 9.05 (sl, 1H, H_8), 8.68 (sl, 1H, H_4), 8.30 (s, 1H, H_2), 8.16-8.01 (m, 3H, H_{15}, H_{16} and H_6), 7.68-7.66 (m, 2H, H_{14} and H_{17}), 7.49 (sl, 1H, H_5), 5.58 (s, 2H, H_{10}), 5.08 (t, 1H, *J* = 7.0 Hz, H_{22}), 3.28 (d, 2H, *J* = 7.0 Hz, H_{21}), 1.68 (s, 3H, H_{25}), 1.59 (s, 3H, H_{24}). ^{13}C NMR (50 MHz, $CDCl_3$): δ 185.14, 181.94, 155.97, 150.18, 145.33, 141.66, 135.91, 134.01, 133.66, 133.46, 132.06, 131.43, 128.22, 126.42, 126.24, 124.41, 121.77, 119.81, 66.06, 25.86, 23.36, 18.06. HRMS-ESI-IT-TOF: m/z calculated $C_{24}H_{23}N_4O_3$ (M+H) 415.1770, found 415.1665.

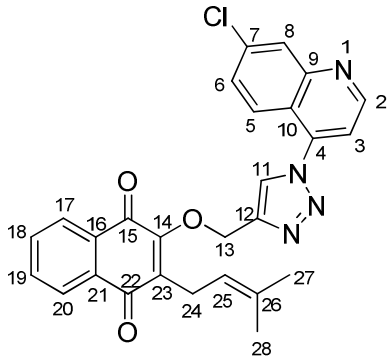

2-((1-(7-Chloroquinolin-4-yl)-1H-*1,2,3*-triazol-4-yl)methoxy)-3-(3-methylbut-2-enyl)naphthalene-1,4-dione

Yield: 78%, mp 130-136 ºC, IR (λ_{max}, cm^{-1}): 3128, 3095, 3053, 2963, 2909, 2852, 2124, 1657, 1610, 1591, 1560, 1505, 1454, 1437, 1332, 1304, 1258, 1236, 1189, 1043, 949, 908, 877, 849, 817, 710. ^{1}H NMR (200 MHz, $CDCl_3$): δ9.04 (d, 1H, J = 4.6 Hz, H_{11}), 8.27 (m, 2H, H_5 and H_2), 8.07.-8.05 (m, 2H, H_{18} and H_{19}), 7.95 (d, 2H, J = 8.6 Hz, H_8), 7.73-7.71 (m, 2H,H_{17} and H_{20}), 7.59-7.55 (m, 2H, H_3 and H_6), 5.68 (s, 2H, H_{13}), 5.09 (t, 1H, J = 6.6 Hz, H_{25}), 3.31 (d, 2H, J = 6.6 Hz, H_{24}), 1.74 (s, 3H, H_{28}), 1.64 (s, 3H, H_{27}). ^{13}C NMR (50 MHz, $CDCl_3$): δ184.89, 181.83, 155.88, 151.31, 150.23, 144.85, 140.85, 136.92, 135.91, 133.89, 133.27, 132.06, 131.39, 129.43, 129.03, 126.33, 126.09, 125.26, 124.37, 120.59, 119.74, 116.01, 65.98, 25.66, 23.29, 17.92. HRMS-ESI-IT-TOF: m/z calculated $C_{27}H_{21}ClN_4O_3Na$ (M+Na) 507.1200, found 507.1917.

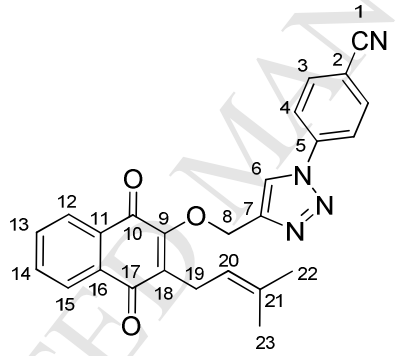

4-(4-((3-(3-Methylbut-2-enyl)-1,4-dioxo-1,4-dihydronaphthalen-2-yloxy)methyl)-1H-*1,2,3*-triazol-1-yl)benzonitrile

Yield: 46%, mp 170-175 ºC, IR (λ_{max}, cm^{-1}): 3151, 3052, 2911, 2233, 1655, 1606, 1593, 1502, 1442, 1373, 1350, 1331, 1259, 1238, 1192, 1143, 1046, 949, 921, 896, 844, 833, 791, 781, 700.^{1}H NMR (200 MHz, $CDCl_3$): δ8.28 (s, 1H,H_6), 8.09-8.08 (m, 2H, H_{12} and H_{13}), 7.97-7.87 (m, 4H,H_3 and H_4), 5.68 (s, 2H, H_8), 5.05 (t, 1H, J = 7.2 Hz, H_{20}), 3.31 (d, 2H, J = 6.0 Hz, H_{19}), 1.73 (s, 3H, H_{23}), 1.64 (s, 3H, H_{22}). ^{13}C NMR (50 MHz, $CDCl_3$): δ184.92, 181.83, 155.85, 145.54, 139.74, 135.92, 133.91, 133.29, 132.08, 131.41, 126.35, 126.11, 125.89, 121.27, 120.63, 119.74, 117.52, 112.68, 65.98, 25.66, 23.26, 17.91. HRMS-ESI-IT-TOF: m/z calculated $C_{25}H_{20}N_4O_3Na$ (M+Na) 447.1433, found 447.1907.

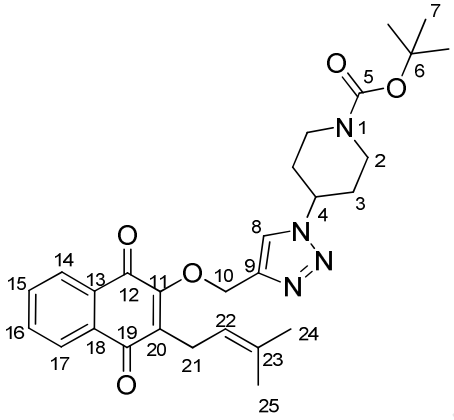

Tert-butyl 4-(4-((3-(3-methylbut-2-enyl)-1,4-dioxo-1,4-dihydronaphthalen-2-yloxy)methyl)-1H-*1,2,3*-triazol-1-yl)piperidine-1-carboxylate

Yield: 41%, mp 100-107 ºC, IR (λ_{max}, cm^{-1}): 3130, 3051, 2974, 2925, 2094, 1683, 1667, 1654, 1605, 1578, 1454, 1402, 1365, 1333, 1274, 1259, 1237, 1192, 1166, 1117, 1049, 1019, 948, 934, 849, 819, 771, 708, 662. ^{1}H NMR (200 MHz, $CDCl_3$): δ 8.08-8.04 (m, 2H, H_{15} and H_{16}), 7.79 (s, 1H,H_8), 7.72-7.68 (m, 2H, H_{14} and H_{17}), 5.51 (s, 2H, H_{10}), 5.03 (t, 1H, J = 6.6 Hz, H_{22}), 4.65-4.58 (m, 1H, H_4), 4.30-4.24 (m, 2H, H_2), 3.24 (d, 2H, J = 6.6 Hz, H_{21}), 2.95 (t, 2H, J = 12.4 Hz, H_3), 1.70 (s, 3H, H_{25}), 1.64 (s, 3H, H_{24}), 1.48 (s, 13H, H_6 and H_7). ^{13}C NMR (50 MHz, $CDCl_3$): δ 185.00, 181.80, 156.06, 154.43, 135.73, 133.76, 133.61, 133.18, 132.08, 131.47, 126.24, 126.06, 119.83, 80.10, 66.32, 58.23, 42.54, 32.36, 30.56, 28.36, 25.64, 23.22, 17.86. HRMS-ESI-IT-TOF: m/z calculated $C_{28}H_{34}N_4O_3Na$ (M+Na) 529.2427, found 529.2432.

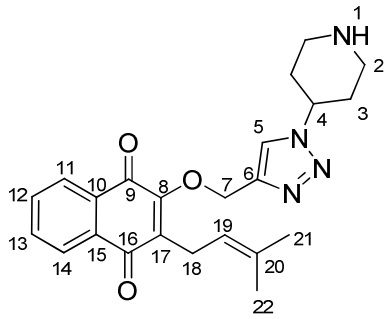

2-(3-Methylbut-2-enyl)-3-((1-(piperidin-4-yl)-1H-*1,2,3*-triazol-4-yl)methoxy)naphthalene-1,4-dione

To a solution of compound **4** (50 mg, 0.1 mmol) in 3 mL of diethyl ether and 0.1 mL of methanol, was added a solution of hydrogen chloride 1 M (2 mL) and stirred at room temperature for 5 minutes. Product was washed with sat. $NaHCO_3$(aq) (3 x 5 mL), dried over Na_2SO_4 and concentrated in vacuum to afford a viscous orange oil as product.

Yield: 25%, mp 115.9-120.3 ºC, IR (λ_{max}, cm^{-1}): 3049, 3006, 2924, 1670, 1422, 1365, 1238, 1156, 1002, 943, 855, 767. ^{1}H NMR (200 MHz, $CDCl_3$): δ 8.28 (s, 1H,H_6), 8.09-8.08 (m, 2H, H_{12} and H_{13}), 7.97-7.87 (m, 4H,H_3 and H_4), 5.68 (s, 2H, H_8), 5.05 (t, 1H, J = 7.2 Hz, H_{20}), 3.31 (d, 2H, J = 6.0 Hz, H_{19}), 1.73 (s, 3H, H_{23}), 1.64 (s, 3H, H_{22}). ^{13}C NMR (50 MHz, $CDCl_3$): δ 185.00, 181.81, 155.45, 135.74, 133.75, 133.61, 133.19, 131.47, 126.23, 126.06, 119.84, 80.12, 66.29, 58.21, 42.53, 32.34, 30.55, 28.35, 25.62, 23.22, 17.84. HRMS-ESI-IT-TOF: m/z calculated $C_{23}H_{27}N_4O_3$ (M+H) 407.2083, found 407.2187.

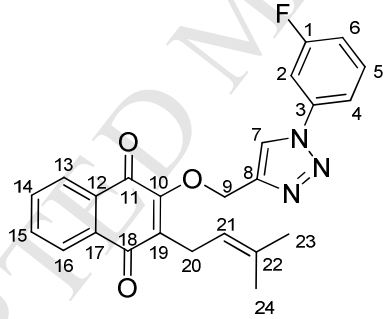

2-((1-(3-Fluorophenyl)-1H-*1,2,3*-triazol-4-yl)methoxy)-3-(3-methylbut-2-enyl)naphthalene-1,4-dione

Yield: 34%, mp 33-35 ºC, IR (λ_{max}, cm^{-1}): 3056, 3046, 2918, 2850, 1668, 1652, 1606, 1500, 1484, 1459, 1373, 1351, 1332, 1260, 1339, 1205, 1189, 1142, 1048, 952, 869, 781, 710, 677. ^{1}H NMR (200 MHz, $CDCl_3$): δ 8.19 (s, 1H,H_7), 8.09-8.08 (m, 2H, H_{14} and H_{15}), 7.73-7.71 (m, 2H, H_{13} and H_{16}), 7.53 (sl, 3H, H_2, H_4 and H_6), 7.16 (t, 1H, J = 7.4 Hz, H_5), 5.61 (s, 2H, H_9), 5.07 (t, 1H, J = 6.2 Hz, H_{21}), 3.29 (d, 2H, J = 6.2 Hz, H_{20}), 1.72 (s, 3H, H_{24}), 1.64 (s, 3H, H_{23}). ^{13}C NMR (50 MHz, $CDCl_3$): δ 184.97, 181.85, 155.95, 144.97, 138.26, 138.05, 135.86, 133.83, 133.79, 133.23, 132.12, 131.48, 131.30, 131.11, 126.31, 126.12, 121.46, 119.82, 115.88, 115.83, 115.53,

108.61, 108.08, 66.07, 29.64, 25.64, 23.27, 17.90, 15.21. HRMS-ESI-IT-TOF: m/z calculated $C_{24}H_{20}FN_3O_3Na$ (M+Na) 440.1386, found 440.1154.

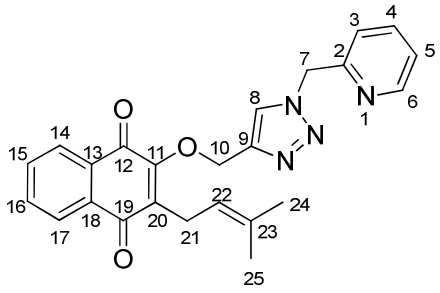

2-(3-Methylbut-2-enyl)-3-((1-(pyridin-2-ylmethyl)-1H-*1,2,3*-triazol-4-yl)methoxy)naphthalene-1,4-dione

Yield: 37%, mp 125-130 ºC, IR (λ_{max}, cm^{-1}): 3131, 3049, 2923, 1651, 1607, 1606, 1591, 1476, 1456, 1437, 1347,1330, 1307, 1264, 1244, 1224, 1192, 1154, 1053, 1029, 994, 952, 921, 845, 827, 792, 767, 747, 706, 690, 661. ^{1}H NMR (200 MHz, $CDCl_3$): δ8.56 (s, 1H,H_8), 8.05-8.04 (m, 2H, H_{15} and H_{16}), 7.86 (sl, 1H, H_6), 7.69-7.62 (m, 3H, H_4, H_{14} and H_{17}), 7.18-7.14 (m, 2H, H_3 and H_5), 5.66 (s, 2H, H_{10}), 5.55 (s, 2H, H_7), 5.00 (t, 1H, J = 6.4 Hz, H_{22}), 3.19 (d, 2H, J = 6.4 Hz, H_{21}), 1.66 (s, 3H, H_{25}), 1.61 (s, 3H, H_{24}). ^{13}C NMR (50 MHz, $CDCl_3$): δ184.99, 181.81, 155.92, 154.32, 148.70, 137.37, 137.22, 135.82, 133.70, 133.57, 133.15, 132.07, 131.47, 126.19, 126.08, 124.01, 123.35, 122.30, 119.80, 66.10, 55.62, 25.60, 23.20, 17.83. HRMS-ESI-IT-TOF: m/z calculated $C_{24}H_{22}N_4O_3Na$ (M+Na) 437.1590, found 437.1685.

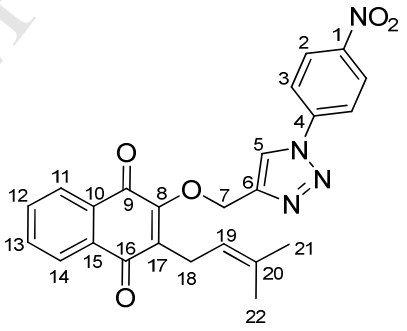

2-(3-Methylbut-2-enyl)-3-((1-(4-nitrophenyl)-1H-*1,2,3*-triazol-4-yl)methoxy)naphthalene-1,4-dione

Yield: 76%, mp 140-145 ºC, IR (λ_{max}, cm^{-1}): 3152, 3019, 2921, 1713, 1659, 1600, 1596, 1523, 1341, 1258, 1194, 1110, 1059, 1045, 1017, 989, 949, 820, 796, 749, 684. ^{1}H NMR (200 MHz, $CDCl_3$): δ 8.45 (s, 1H,H_5), 8.39 (d, 2H, H_2), 8.08-8.00 (m, 4H, H_3, H_{12} and H_{13}), 7.73-7.71 (m, 2H, H_{11} and H_{14}), 5.61 (s, 2H, H_7), 5.05 (t, 1H, J = 7.0 Hz, H_{19}), 3.29 (d, 2H, J = 7.0 Hz, H_{18}), 1.72 (s, 3H, H_{22}), 1.63 (s, 3H, H_{21}). ^{13}C NMR (50 MHz, $CDCl_3$): δ 184.89, 181.82, 155.85, 147.461, 145.68, 141.08, 135.89, 133.91, 133.85, 133.28, 132.07, 131.40, 126.33, 126.09, 125.49, 121.47, 120.55, 119.74, 65.93, 25.63, 23.25, 17.86. HRMS-ESI-IT-TOF: m/z calculated $C_{24}H_{20}N_4O_5Na$ (M+Na) 467.1331, found 467.1100.

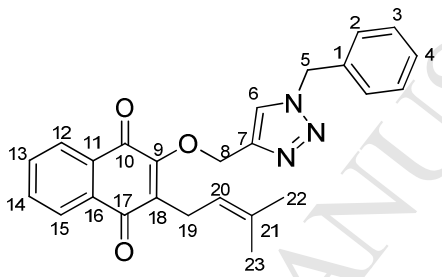

2-((1-Benzyl-1H-*1*,*2*,*3*-triazol-4-yl)methoxy)-3-(3-methylbut-2-enyl)naphthalene-1,4-dione

Yield: 81%, mp 94-100 ºC, IR (λ_{max}, cm^{-1}): 3117, 3074, 3033, 2924, 1664, 1631, 1592, 1515, 1497, 1369, 1331, 1239, 1191, 1056, 1045, 1035, 951, 931, 8494, 818, 818. ^{1}H NMR (200 MHz, $CDCl_3$): δ 8.10 (s, 1H, H_6), 8.08-8.04 (m, 2H, H_{13} and H_{14}), 7.71-7.61 (m, 4H, H_3, H_{12} and H_{15}), 7.04-6.99 (m, 3H, H_2 and H_4), 5.60 (s, 2H, H_8), 5.04 (t, 1H, J = 7.2 Hz, H_{20}), 3.86 (s, 2H, H_5), 3.30 (d, 2H, J = 7.2 Hz, H_{19}), 1.71 (s, 3H, H_{23}), 1.62 (s, 3H, H_{22}). ^{13}C NMR (50 MHz, $CDCl_3$): δ 185.01, 181.85, 160.00, 156.04, 144.40, 135.79, 133.76, 133.67, 133.18, 132.12, 131.52, 130.47, 126.26, 126.10, 122.20, 121.65, 119.87, 114.85, 66.20, 55.60, 25.63, 23.27, 17.88. HRMS-ESI-IT-TOF: m/z calculated $C_{25}H_{24}N_3O_3$ (M+H) 414.1818, found 414.2003.

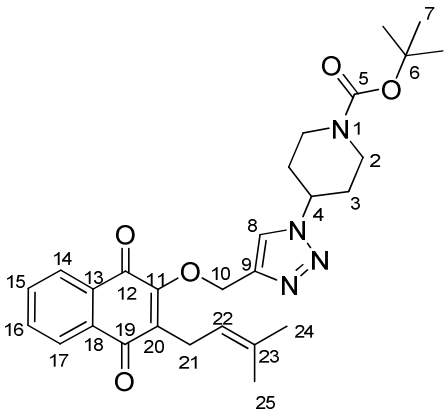

Tert-butyl 4-(4-((3-(3-methylbut-2-enyl)-1,4-dioxo-1,4-dihydronaphthalen-2-yloxy)methyl)-1H-*1,2,3*-triazol-1-yl)piperidine-1-carboxylate

Yield: 41%, mp 100-107 ºC, IR (λ_{max}, cm^{-1}): 3151, 3050, 2974, 2925, 2094, 1683, 1667, 1654, 1605, 1578, 1454, 1402, 1365, 1333, 1274, 1259, 1237, 1192, 1166, 1117, 1049, 1019, 948, 934, 849, 819, 771, 708, 662. ^{1}H NMR (200 MHz, $CDCl_3$): δ 8.08-8.04 (m, 2H, H_{15} and H_{16}), 7.79 (s, 1H,H_8), 7.72-7.68 (m, 2H, H_{14} and H_{17}), 5.51 (s, 2H, H_{10}), 5.03 (t, 1H, J = 6.6 Hz, H_{22}), 4.65-4.58 (m, 1H, H_4), 4.30-4.24 (m, 2H, H_2), 3.24 (d, 2H, J = 6.6 Hz, H_{21}), 2.95 (t, 2H, J = 12.4 Hz, H_3), 1.70 (s, 3H, H_{25}), 1.64 (s, 3H, H_{24}), 1.48 (s, 13H, H_6 and H_7). ^{13}C NMR (50 MHz, $CDCl_3$): δ185.00, 181.80, 156.06, 154.43, 135.73, 133.76, 133.61, 133.18, 132.08, 131.47, 126.24, 126.06, 119.83, 80.10, 66.32, 58.23, 42.54, 32.36, 30.56, 28.36, 25.64, 23.22, 17.86. HRMS-ESI-IT-TOF: m/z calculated $C_{28}H_{34}N_4O_3Na$ (M+Na) 529.2427, found 529.2432.

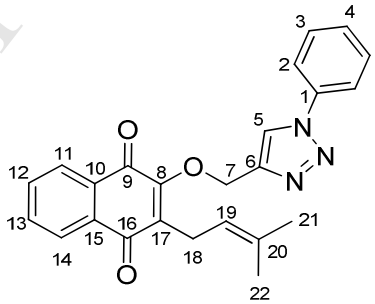

2-(3-Methylbut-2-enyl)-3-((1-phenyl-1H-*1,2,3*-triazol-4-yl)methoxy) naphthalene-1,4-dione

Yield: 59%, mp 89-107 ºC, IR (λ_{max}, cm^{-1}): 3055, 3031, 3002, 2951, 1651, 1592, 1500, 1455, 1332, 1263, 1239, 1188, 1046, 955, 850, 759, 688.^{1}H NMR (200 MHz, $CDCl_3$): δ 8.20 (s,

1H,H_5), 8.09-8.04 (m, 2H, H_{12} and H_{13}), 7.76-7.67 (m, 5H, H_2, H_4, H_{11} and H_{14}), 7.53-7.48 (m, 2H, H_3), 5.62 (s, 2H, H_7), 5.04 (t, 1H, J = 7.4 Hz, H_{19}), 3.28 (d, 2H, J = 7.4 Hz, H_{18}), 1.71 (s, 3H, H_{25}), 1.62 (s, 3H, H_{21}). ^{13}C NMR (50 MHz, $CDCl_3$): δ 185.01, 181.85, 155.99, 136.98, 135.79, 133.79, 133.72, 133.20, 132.09, 131.47, 129.73, 128.83, 126.26, 126.10, 121.54, 120.56, 119.82, 66.12, 25.63, 23.25, 17.88. HRMS-ESI-IT-TOF: m/z calculated $C_{24}H_{22}N_3O_3$ (M+H) 400.1661, found 400.1580.

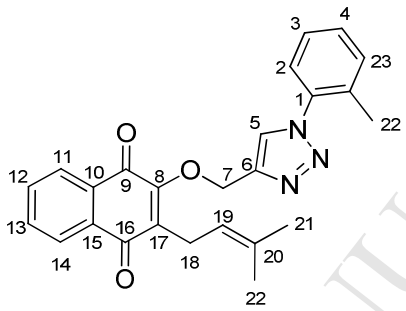

2-(3-Methylbut-2-en-1-yl)-3-((1-(o-tolyl)-1H-*1,2,3*-triazol-4-yl)methoxy)naphthalene-1,4-dione

Yield: 63%, mp 59-60 ºC, IR (λ_{max}, cm^{-1}): 3117, 3074, 3033, 2924, 2883, 1664, 1651, 1609, 1592, 1578, 1455, 1439, 1375, 1336, 1300, 1261, 1238, 1193, 1127, 1029, 1010, 986, 948, 929, 849, 818, 802, 795, 778, 768, 740, 700, 675, 661. ^{1}H NMR (300 MHz, $CDCl_3$): δ 8.09-8.06 (m, 3H, H_5, H_{12} and H_{13}), 7.72-7.70 (m, 2H, H_{11} and H_{14}), 7.42-7.27 (m, 4H, H_2, H_3, H_4, H_{23}), 5.64 (s, 2H, H_7), 5.07 (t, 1H, J = 7.4 Hz, H_{19}), 3.28 (d, 2H, J = 7.4 Hz, H_{18}), 2.19 (s, 3H, H_{22}), 1.72 (s, 3H, H_{21}), 1.64 (s, 3H, H_{21}). ^{13}C NMR (75 MHz, $CDCl_3$): δ 185.21, 181.96, 156.02, 143.72, 136.32, 135.38, 133.94, 133.67, 133.39, 133.34, 132.02, 131.55, 131.50, 131.40, 130.07, 130.03, 126.91, 126.31, 126.21, 119.71, 66.18, 25.82, 23.25, 17.86, 17.79. HRMS-ESI-IT-TOF: m/z calculated $C_{25}H_{24}N_3O_3$ (M+H) 414.1739, found 414.1310.

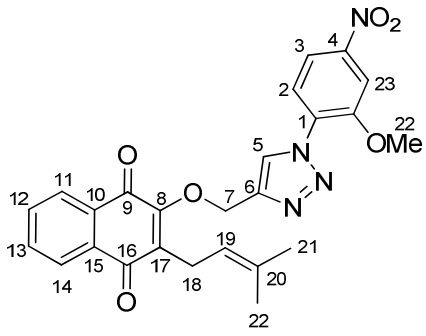

2-((1-(2-Methoxy-4-nitrophenyl)-1H-*1,2,3*-triazol-4-yl)methoxy)-3-(3-methylbut-2-enyl)naphthalene-1,4-dione

Yield: 55%, mp 229-236 ºC, IR (λ_{max}, cm^{-1}): 3152, 2921, 1713, 1659, 1600, 1525, 1503, 1457, 1341, 1265, 1231, 1185, 1140, 1096, 1048, 1018, 950, 903, 883, 828, 799, 743, 728. ^{1}H NMR (200 MHz, $CDCl_3$): δ8.68 (s, 1H,H_5), 8.34-8.32 (m, 2H, H_{12} and H_{13}), 8.28-8.24 (m, 2H, H_2, H_3), 8.02-8.00 (m, 2H, H_{11} and H_{14}) 7.22-7.14 (m, 1H, H_{23}), 5.61 (s, 2H, H_7), 5.10 (t, 1H, *J* = 7.8 Hz, H_{19}), 3.24 (d, 2H, *J* = 7.8 Hz, H_{18}), 1.57 (s, 3H, H_{22}), 1.59 (s, 3H, H_{21}). ^{13}C NMR (50 MHz, $CDCl_3$): δ 184.89, 181.71, 155.69, 136.45, 141.26, 135.69, 133.78, 133.64, 133.18, 131.83, 131.22, 126.11, 125.96, 125.57, 125.45, 120.96, 119.56, 65.77, 56.91, 25.57, 23.11, 17.77. HRMS-ESI-IT-TOF: m/z calculated $C_{25}H_{23}N_4O_6$ (M+H) 475.1618, found 475.1580.

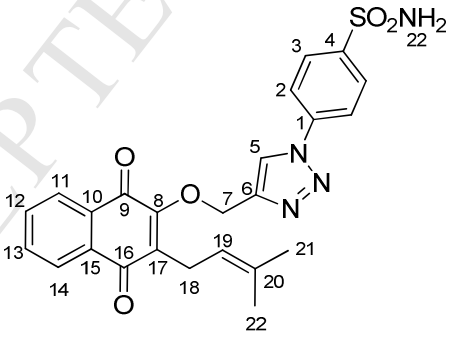

4-(4-(((3-(3-methylbut-2-en-1-yl)-1,4-dioxo-1,4-dihydronaphthalen-2-yl)oxy)methyl)-1H-*1,2,3*-triazol-1-yl)benzenesulfonamide

Yield: 76%, mp 198-200 ºC, IR (λ_{max}, cm^{-1}): 3241, 3071, 2929, 2850, 1660, 1623, 1592, 1455, 1386, 1262, 1240, 1197, 1112, 1095, 1050, 995, 949, 834, 904, 850, 798, 786, 722, 661. ^{1}H NMR (300 MHz, DMSO-d_6): ^{1}H NMR (300 MHz, DMSO-d_6): δ9.08 (s, 1H,H_5), 8.16-8.13 (m,

2H, H_{12} and H_{13}), 8.04-8.01 (m, 2H, H_2), 7.98-7.85 (m, 2H, H_3), 7.57-7.55 (m, 2H, H_{11} and H_{14}), 5.58 (s, 2H, H_7), 4.83 (t, 1H, J = 6.0 Hz, H_{19}), 3.09, (d, 2H, J = 6.0 Hz, H_{18}), 1.98 (sl, 2H, NH_2) 1.57 (s, 3H, H_{22}), 1.47 (s, 3H, H_{21}). ^{13}C NMR (75 MHz, DMSO-d_6): δ 185.10, 181.56, 156.50, 144.55, 144.38, 138.93, 134.88, 134.69, 134.37, 132.97, 131.84, 131.66, 128.02, 126.47, 126.24, 123.75, 120.75, 120.39, 65.62, 25.84, 23.11, 18.10. HRMS-ESI-IT-TOF: m/z calculated $C_{24}H_{23}N_4O_5S$ (M+H) 479.1389, found 479.3354.

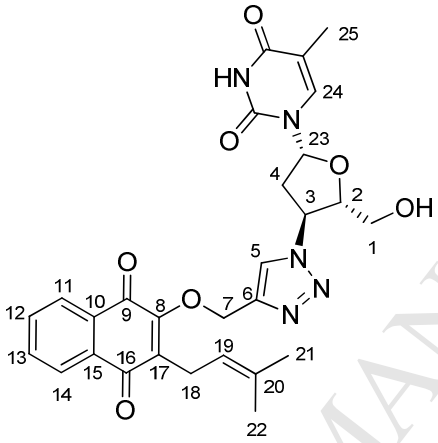

1-((2R,4S,5S)-5-(hydroxymethyl)-4-(4-(((3-(3-methylbut-2-en-1-yl)-1,4-dioxo-1,4-dihydronaphthalen-2-yl)oxy)methyl)-1H-1,2,3-triazol-1-yl)tetrahydrofuran-2-yl)-5-methylpyrimidine-2,4(1H,3H)-dione

Yield: 42%, mp 178-185 ºC, IR (λ_{max}, cm^{-1}): 3241, 3071, 2929, 2850, 1660, 1623, 1592, 1455, 1386,1262, 1240, 1197, 1112, 1095, 1050, 995, 949, 834, 904, 850, 798, 786, 722, 661. ^{1}H NMR (400 MHz, DMSO-d_6): δ 8.21 (s, 1H, H_5), 8.09-8.06 (m, 2H, H_{12} and H_{13}), 7.76-7.70 (m, 2H, $H_{11,}$ H_{14}) 7.56-7.26 (m, 1H, H_{24}), 5.62-5.61 (m, 1H, H_{23}), 5.04-5.02 (m, 3H, $H_{7,}$ H_{19}), 3.88-3.84 (m, 1H, H_3), 3.65-3.61 (m, 2H, $H_{2,}$ -OH), 3.30-3.28 (m, 2H, H_1), 1.72-1.61 (m, 4H, H_4, H_{18}), 1.71 (s, 3H, H_{25}), 1.62 (s, 3H, H_{21}), 1.24 (s, 3H, H_{22}). ^{13}C NMR (100 MHz, DMSO-d_6): δ 185.21, 181.99, 156.02, 144.68, 136.92, 135.92, 133.97, 133.37, 132.08, 131.46, 129.85, 129.04, 126.38, 126.22, 121.77, 120.68, 119. 76, 104.27, 66.10, 63.94, 58.51, 25.72, 23.30, 17.94, 15.32. HRMS-ESI-IT-TOF: m/z calculated $C_{28}H_{30}N_5O_7$ (M+) 548.2145, found 548.4600.

4.4. Molecular modeling

The molecular modeling studies were accomplished using the Schrödinger Small Molecule Drug Discovery Suite (version 2015-3) [55]. The X-ray crystal structure of *Pf*DHODH with a bound inhibitor A26 (PDB-ID: 1TV5) [22] was retrieved from the Protein Data Bank and prepared using Schrödinger's Protein Preparation Wizard (PPW) [56] by adding hydrogens, predicting missing amino acids or side chains, adding caps to C- and N-termini, removing water molecules beyond 5 Å from the bound ligand A26, assigning partial charges using the OPLS–AA 2005 (optimized potentials for liquid simulations – all atoms 2005) force field and finally by running a rapid constrained energy minimization. Ligands were sketched in Maestro [57], studied for any ionization states or possible tautomer(s) and energy minimized using LigPrep [58]. Energy-minimized ligands and protein were used in the Induced Fit [59] docking protocol using the Standard Precision (SP) docking mode, which has been shown to be a reliable approach [60]. The docking score reported is the Glide score. All the possible tautomers of each compound were used in docking. For example, for Lapachol (**1**) the oxy form (O–) displayed the best docking score, and hence its score was reported in this work and that form was included in **Figure 2**. The docking site (receptor grid) was defined using the co-crystalized *Pf*DHODH inhibitor; amino acids within 7 Å of the docked ligand were allowed to be flexible during Glide docking and optimized using the Prime tool simultaneously, in accordance with the InducedFit docking protocol. Other co-crystalized ligands FMN (flavin mononucleotide) and ORO (orotate) in the crystal structure were kept rigid. Visualization and graphics were done in Maestro.

4.5. Acknowledgment

Thanks to Dr. J. R. Stehmann, Departamento de Botânica, Instituto de Ciências Biológicas, UFMG, Belo Horizonte, Brazil, for taxonomic identification of *H. serratifolius*. This work was supported by funds from FAPEMIG – Fundação de Amparo à Pesquisa de Minas Gerais (Brazil), CAPES - Coordenação e Aperfeiçoamento de Pessoal de Nível Superior (Brazil) and CNPq-Conselho Nacional de Desenvolvimento Científico e Tecnológico (Brazil) for financial support to ABO through PRONEX Rede Malária Processes No. APQ-01129-10 and Process 555655/.2009-1, and GRP to Process numbers FIP 2013/8322-2S, APQ 00050-014 and GCB to Process number APQ 01529-15, respectively, and scholarships provided from FAPEMIG, CAPES and CNPq to Alaíde Braga de Oliveira, Geraldo Célio Brandão, Guilherme Rocha Pereira and Franciele Caroline R. Missias are also acknowledged for undergraduate student Jéssica Chequer dos Santos from PUC Minas. This investigation was conducted in part in a facility constructed with support from the Research Facilities Improvements Program (C06-RR14503) from the National Institutes of Health (NIH) National Center for Research Resources.

5. References

[1] R.W. Snow, C.A. Guerra, A.M. Noor, H.Y. Myint, S.I. Hay, The global distribution of clinical episodes of Plasmodium falciparum malaria, Nature, 434 (2005) 214-217.

[2] World Malaria Report 2016, World Health Organizations, Geneva.

[3] L.M.B. Ursos, P.D. Roepe, Chloroquine resistance in the malarial parasite, Plasmodium falciparum, Medicinal Research Reviews, 22 (2002) 465-491.

[4] A.M. Dondorp, F. Nosten, P. Yi, D. Das, A.P. Phyo, J. Tarning, K.M. Lwin, F. Ariey, W. Hanpithakong, S.J. Lee, P. Ringwald, K. Silamut, M. Imwong, K. Chotivanich, P. Lim, T.

Herdman, S.S. An, S. Yeung, P. Singhasivanon, N.P.J. Day, N. Lindegardh, D. Socheat, N.J. White, Artemisinin Resistance in Plasmodium falciparum Malaria (vol 361, pg 455, 2009), New England Journal of Medicine, 361 (2009) 1714-1714.

[5] V.F. de Andrade-Neto, M.O.F. Goulart, J.F. da Silva, M.J. da Silva, M.D. Pinto, A.V. Pinto, M.G. Zalis, L.H. Carvalho, A.U. Krettli, Antimalarial activity of phenazines from lapachol, beta-lapachone and its derivatives against Plasmodium falciparum in vitro and Plasmodium berghei in vivo, Bioorganic & Medicinal Chemistry Letters, 14 (2004) 1145-1149.

[6] A. Riffel, L.F. Medina, V. Stefani, R.C. Santos, D. Bizani, A. Brandelli, In vitro antimicrobial activity of a new series of 1,4-naphthoquinones, Brazilian Journal of Medical and Biological Research, 35 (2002) 811-818.

[7] I.L. Cockburn, A. Boshoff, E.R. Pesce, G.L. Blatch, Selective modulation of plasmodial Hsp70s by small molecules with antimalarial activity, Biological Chemistry, 395 (2014) 1353-1362.

[8] R.A.S. Oliveira, E. Azevedo-Ximenes, R. Luzzati, R.C. Garcia, The hydroxy-naphthoquinone lapachol arrests mycobacterial growth and immunomodulates host macrophages, International Immunopharmacology, 10 (2010) 1463-1473.

[9] I. Caballero, M.J. Lafuente, F.J. Gamo, C. Cid, A high-throughput fluorescence-based assay for Plasmodium dihydroorotate dehydrogenase inhibitor screening, Analytical Biochemistry, 506 (2016) 13-21.

[10] V.F. De Andrade-Neto, M.O.F. Goulart, J.F. Da Silva Filho, M.J. Da Silva, M.D.C.F.R. Pinto, A.V. Pinto, M.G. Zalis, L.H. Carvalho, A.U. Krettli, Antimalarial activity of phenazines

from lapachol, β-lapachone and its derivatives against Plasmodium falciparum in vitro and Plasmodium berghei in vivo, Bioorganic and Medicinal Chemistry Letters, 14 (2004) 1145-1149.

[11] H. Hussain, K. Krohn, V.U. Ahmad, G.A. Miana, I.R. Green, Lapachol: An overview, Arkivoc, 2007 (2007) 145-171.

[12] D.R.M. Moreira, M.S. De Sá, T.S. Macedo, M.N. Menezes, J.R.M. Reys, A.E.G. Santana, T.L. Silva, G.L.A. Maia, J.M. Barbosa-Filho, C.A. Camara, T.M.S. Da Silva, K.N. Da Silva, E.T. Guimaraes, R.R. Dos Santos, M.O.F. Goulart, M.B.P. Soares, Evaluation of naphthoquinones identified the acetylated isolapachol as a potent and selective antiplasmodium agent, Journal of Enzyme Inhibition and Medicinal Chemistry, 30 (2015) 615-621.

[13] A.L. Baggish, D.R. Hill, Antiparasitic agent atovaquone, Antimicrobial Agents and Chemotherapy, 46 (2002) 1163-1173.

[14] J.D. Berman, R. Nielsen, J.D. Chulay, M. Dowler, K.C. Kain, K.E. Kester, J. Williams, A.C. Whelen, M.J. Shmuklarsky, Causal prophylactic efficacy of atovaquone-proguanil (Malarone (TM)) in a human challenge model, Transactions of the Royal Society of Tropical Medicine and Hygiene, 95 (2001) 429-432.

[15] J.L. Guler, J. White, III, M.A. Phillips, P.K. Rathod, Atovaquone Tolerance in Plasmodium falciparum Parasites Selected for High-Level Resistance to a Dihydroorotate Dehydrogenase Inhibitor, Antimicrobial Agents and Chemotherapy, 59 (2015) 686-689.

[16] M.W. Mather, E. Darrouzet, M. Valkova-Valchanova, J.W. Cooley, M.T. McIntosh, F. Daldal, A.B. Vaidya, Uncovering the molecular mode of action of the antimalarial drug atovaquone using a bacterial system, Journal of Biological Chemistry, 280 (2005) 27458-27465.

[17] T. Rodrigues, F. Lopes, R. Moreira, Inhibitors of the Mitochondrial Electron Transport Chain and de novo Pyrimidine Biosynthesis as Antimalarials: The Present Status, Current Medicinal Chemistry, 17 (2010) 929-956.

[18] M.A. Phillips, P.K. Rathod, Plasmodium dihydroorotate dehydrogenase: a promising target for novel anti-malarial chemotherapy, Infectious disorders drug targets, 10 (2010) 226-239.

[19] D.E. Hurt, J. Widom, J. Clardy, Structure of Plasmodium falciparum dihydroorotate dehydrogenase with a bound inhibitor, Acta Crystallographica Section D-Biological Crystallography, 62 (2006) 312-323.

[20] M.T. Makler, J.M. Ries, J.A. Williams, J.E. Bancroft, R.C. Piper, B.L. Gibbins, D.J. Hinrichs, Parasite lactate-dehydrogenase as an assay for plasmodium-falciparum drug-sensitivity, American Journal of Tropical Medicine and Hygiene, 48 (1993) 739-741.

[21] M.L. Booker, C.M. Bastos, M.L. Kramer, R.H. Barker, Jr., R. Skerlj, A.B. Sidhu, X. Deng, C. Celatka, J.F. Cortese, J.E. Guerrero Bravo, K.N. Crespo Llado, A.E. Serrano, I. Angulo-Barturen, M.B. Jimenez-Diaz, S. Viera, H. Garuti, S. Wittlin, P. Papastogiannidis, J.W. Lin, C.J. Janse, S.M. Khan, M. Duraisingh, B. Coleman, E.J. Goldsmith, M.A. Phillips, B. Munoz, D.F. Wirth, J.D. Klinger, R. Wiegand, E. Sybertz, Novel inhibitors of Plasmodium falciparum dihydroorotate dehydrogenase with anti-malarial activity in the mouse model, The Journal of biological chemistry, 285 (2010) 33054-33064.

[22] X. Deng, D. Matthews, P.K. Rathod, M.A. Phillips, The X-ray structure of Plasmodium falciparum dihydroorotate dehydrogenase bound to a potent and selective N-phenylbenzamide

inhibitor reveals novel binding-site interactions, Acta crystallographica. Section F, Structural biology communications, 71 (2015) 553-559.

[23] X. Deng, R. Gujjar, F. El Mazouni, W. Kaminsky, N.A. Malmquist, E.J. Goldsmith, P.K. Rathod, M.A. Phillips, Structural plasticity of malaria dihydroorotate dehydrogenase allows selective binding of diverse chemical scaffolds, The Journal of biological chemistry, 284 (2009) 26999-27009.

[24] P.A. Stocks, V. Barton, T. Antoine, G.A. Biagini, S.A. Ward, P.M. O'Neill, Novel inhibitors of the Plasmodium falciparum electron transport chain, Parasitology, 141 (2014) 50-65.

[25] A. Manhas, M.Y. Lone, P.C. Jha, Multicomplex-based pharmacophore modeling coupled with molecular dynamics simulations: An efficient strategy for the identification of novel inhibitors of PfDHODH, Journal of Molecular Graphics and Modelling, 75 (2017) 413-423.

[26] E. Pavadai, F. El Mazouni, S. Wittlin, C. De Kock, M.A. Phillips, K. Chibale, Identification of New Human Malaria Parasite Plasmodium falciparum Dihydroorotate Dehydrogenase Inhibitors by Pharmacophore and Structure-Based Virtual Screening, Journal of Chemical Information and Modeling, 56 (2016) 548-562.

[27] J. Zhu, L. Han, Y. Diao, X. Ren, M. Xu, L. Xu, S. Li, Q. Li, D. Dong, J. Huang, X. Liu, Z. Zhao, R. Wang, L. Zhu, Y. Xu, X. Qian, H. Li, Design, Synthesis, X-ray Crystallographic Analysis, and Biological Evaluation of Thiazole Derivatives as Potent and Selective Inhibitors of Human Dihydroorotate Dehydrogenase, Journal of Medicinal Chemistry, 58 (2015) 1123-1139.

[28] M.L. Bolognesi, F. Lizzi, R. Perozzo, R. Brun, A. Cavalli, Synthesis of a small library of 2-phenoxy-1,4-naphthoquinone and 2-phenoxy-1,4-anthraquinone derivatives bearing anti-

trypanosomal and anti-leishmanial activity, Bioorganic & Medicinal Chemistry Letters, 18 (2008) 2272-2276.

[29] K. Singh, H. Kaur, K. Chibale, J. Balzarini, S. Little, P.V. Bharatam, 2-Aminopyrimidine based 4-aminoquinoline anti-plasmodial agents. Synthesis, biological activity, structure-activity relationship and mode of action studies, European Journal of Medicinal Chemistry, 52 (2012) 82-97.

[30] N. Sunduru, M. Sharma, K. Srivastava, S. Rajakumar, S.K. Puri, J.K. Saxena, P.M.S. Chauhan, Synthesis of oxalamide and triazine derivatives as a novel class of hybrid 4-aminoquinoline with potent antiplasmodial activity, Bioorganic & Medicinal Chemistry, 17 (2009) 6451-6462.

[31] H.C. Kolb, M.G. Finn, K.B. Sharpless, Click chemistry: Diverse chemical function from a few good reactions, Angewandte Chemie-International Edition, 40 (2001) 2004-+.

[32] T.A. Bakka, M.B. Strøm, J.H. Andersen, O.R. Gautun, Methyl propiolate and 3-butynone: Starting points for synthesis of amphiphilic 1,2,3-triazole peptidomimetics for antimicrobial evaluation, Bioorganic and Medicinal Chemistry, 25 (2017) 5380-5395.

[33] T.A. Bakka, M.B. Strøm, J.H. Andersen, O.R. Gautun, Synthesis and antimicrobial evaluation of cationic low molecular weight amphipathic 1,2,3-triazoles, Bioorganic and Medicinal Chemistry Letters, 27 (2017) 1119-1123.

[34] T.B. Cassamale, E.C. Costa, D.B. Carvalho, N.S. Cassemiro, C.C. Tomazela, M.C.S. Marques, M. Ojeda, M.F.C. Matos, S. Albuquerque, C.C.P. Arruda, A.C.M. Baroni, Synthesis and Antitrypanosomastid Activity of 1,4-Diaryl-1,2,3-triazole Analogues of Neolignans

Veraguensin, Grandisin and Machilin G, Journal of the Brazilian Chemical Society, 27 (2016) 1217-1228.

[35] C. Darsih, V. Prachyawarakorn, S. Wiyakrutta, C. Mahidol, S. Ruchirawat, P. Kittakoop, Cytotoxic metabolites from the endophytic fungus Penicillium chermesinum: Discovery of a cysteine-targeted Michael acceptor as a pharmacophore for fragment-based drug discovery, bioconjugation and click reactions, RSC Advances, 5 (2015) 70595-70603.

[36] W. Hou, Z. Luo, G. Zhang, D. Cao, D. Li, H. Ruan, B.H. Ruan, L. Su, H. Xu, Click chemistry-based synthesis and anticancer activity evaluation of novel C-14 1,2,3-triazole dehydroabietic acid hybrids, European Journal of Medicinal Chemistry, 138 (2017) 1042-1052.

[37] B. Mistry, R.V. Patel, Y.S. Keum, Access to the substituted benzyl-1,2,3-triazolyl hesperetin derivatives expressing antioxidant and anticancer effects, Arabian Journal of Chemistry, 10 (2017) 157-166.

[38] S. Nickel, R.A. Serwa, F. Kaschani, S. Ninck, S. Zweerink, E.W. Tate, M. Kaiser, Chemoproteomic Evaluation of the Polyacetylene Callyspongynic Acid, Chemistry - A European Journal, 21 (2015) 10721-10728.

[39] R. Yamada, M. Hiraizumi, S. Narita, K. Sakurai, Two-Step Synthesis of a Clickable Photoaffinity Probe from an Anticancer Saponin OSW-1 and its Photochemical Reactivity, Asian Journal of Organic Chemistry, 5 (2016) 330-334.

[40] P.J. Rosenthal, ed., Antimalarial Chemotherapy. Mechanisms of Action, Resistance and New Directions in Drug Discovery, Humana Press, Totowa, NJ.

[41] V.F. Andrade-Neto, M.O. Goulart, J.F. da Silva Filho, M.J. da Silva, C. Pinto Mdo, A.V. Pinto, M.G. Zalis, L.H. Carvalho, A.U. Krettli, Antimalarial activity of phenazines from lapachol, beta-lapachone and its derivatives against *Plasmodium falciparum* in vitro and *Plasmodium berghei* in vivo, Bioorg Med Chem Lett, 14 (2004) 1145-1149.

[42] W. Trager, J.B. Jensen, Human malaria parasites in continuous culture, Science, 193 (1976) 673-675.

[43] H. Noedl, J. Bronnert, K. Yingyuen, B. Attlmayr, H. Kollaritsch, M. Fukuda, Simple histidine-rich protein 2 double-site sandwich enzyme-linked immunosorbent assay for use in malaria drug sensitivity testing, Antimicrob Agents Chemother, 49 (2005) 3575-3577.

[44] H. Noedl, W.H. Wernsdorfer, R.S. Miller, C. Wongsrichanalai, Histidine-rich protein II: a novel approach to malaria drug sensitivity testing, Antimicrob Agents Chemother, 46 (2002) 1658-1664.

[45] C. Lambros, J.P. Vanderberg, Synchronization of *Plasmodium falciparum* erythrocytic stages in culture, J Parasitol, 65 (1979) 418-420.

[46] F.P. Varotti, A.C. Botelho, A.A. Andrade, R.C. de Paula, E.M. Fagundes, A. Valverde, L.M. Mayer, J.S. Mendonca, M.V. de Souza, N. Boechat, A.U. Krettli, Synthesis, antimalarial activity, and intracellular targets of MEFAS, a new hybrid compound derived from mefloquine and artesunate, Antimicrob Agents Chemother, 52 (2008) 3868-3874.

[47] P.R. Twentyman, M. Luscombe, A study of some variables in a tetrazolium dye (MTT) based assay for cell growth and chemosensitivity, Br J Cancer, 56 (1987) 279-285.

[48] J.M. Calvo-Calle, A. Moreno, W.M. Eling, E.H. Nardin, In vitro development of infectious liver stages of *P. yoelii* and *P. berghei* malaria in human cell lines, Exp Parasitol, 79 (1994) 362-373.

[49] M. Madureira, A. Paula Martins, M. Gomes, J. Paiva, A. Proenca da Cunha, V. do Rosario, Antimalarial activity of medicinal plants used in traditional medicine in S. Tome and Principe islands, J Ethnopharmacol, 81 (2002) 23-29.

[50] M.S. Sa, J.F. Costa, A.U. Krettli, M.G. Zalis, G.L. Maia, I.M. Sette, A. Camara Cde, J.M. Filho, A.M. Giulietti-Harley, R. Ribeiro Dos Santos, M.B. Soares, Antimalarial activity of betulinic acid and derivatives in vitro against *Plasmodium falciparum* and in vivo in *P. berghei*-infected mice, Parasitol Res, 105 (2009) 275-279.

[51] A.M. Innocente, G.N. Silva, L.N. Cruz, M.S. Moraes, M. Nakabashi, P. Sonnet, G. Gosmann, C.R. Garcia, S.C. Gnoatto, Synthesis and antiplasmodial activity of betulinic acid and ursolic acid analogues, Molecules, 17 (2012) 12003-12014.

[52] G.R. Pereira, G.C. Brandao, L.M. Arantes, H.A. de Oliveira, Jr., R.C. de Paula, M.F.A. do Nascimento, F.M. dos Santos, R.K. da Rocha, J.C.D. Lopes, A.B. de Oliveira, 7-Chloroquinolinotriazoles: Synthesis by the azide-alkyne cycloaddition click chemistry, antimalarial activity, cytotoxicity and SAR studies, European Journal of Medicinal Chemistry, 73 (2014) 295-309.

[53] J.d.O. Santos, G.R. Pereira, G.C. Brandão, T.F. Borgati, L.M. Arantes, R.C.d. Paula, L.F. Soares, M.F.A.d. Nascimento, M.R.C. Ferreira, A.G. Taranto, F.P. Varotti, A.B.d. Oliveira, Synthesis, in vitro Antimalarial Activity and in silico Studies of Hybrid Kauranoid 1,2,3-

Triazoles Derived from Naturally Occurring Diterpenes, Journal of the Brazilian Chemical Society, 27 (2016) 551-565.

[54] M.V.N. de Souza, K.C. Pais, C.R. Kaiser, M.A. Peralta, M. de L. Ferreira, M.C.S. Lourenço, Synthesis and in vitro antitubercular activity of a series of quinoline derivatives, Bioorganic and Medicinal Chemistry, 17 (2009) 1474-1480.

[55] Small-Molecule Drug Discovery Suite 2015-3: Schrödinger, LLC, in, New York, NY, 2015.

[56] Schrödinger Release 2015-3: Schrödinger Suite 2015-3 Protein Preparation Wizard; Epik version 3.3, Schrödinger, LLC, New York, NY, 2015; Impact version 6.8, Schrödinger, LLC, New York, NY, 2015; Prime version 4.1, Schrödinger, LLC, in, New York, NY, 2015.

[57] Schrödinger Release 2015-3: Maestro, version 10.3, Schrödinger, LLC, in, New York, NY, 2015.

[58] Schrödinger Release 2015-3: LigPrep, version 3.5, Schrödinger, LLC, in, New York, NY, 2015.

[59] Small-Molecule Drug Discovery Suite 2015-3: Schrödinger Suite 2015-3 Induced Fit Docking protocol; Glide version 6.8, Schrödinger, LLC, New York, NY, 2015; Prime version 4.1, Schrödinger, LLC, in, New York, NY, 2015.

[60] G. Fu, P. Sivaprakasam, O.R. Dale, S.P. Manly, S.J. Cutler, R.J. Doerksen, Pharmacophore modeling, ensemble docking, virtual screening, and biological evaluation on glycogen synthase kinase-3β, Molecular Informatics, (2014).

Highlights for the reviewers:

- Revised final manuscript was updated including every review suggestion;
- Authors found small corrections (stereochemistry bond correction in the AZT triazole compound (18) and table numbers that were not alignment);
- New citations were added to support the material;
- Fixed all the references (including removing one accidentally duplicated one) and updated all of their formatting;
- We fixed some of the entries in Table 2;
- We corrected the caption to Figure 3, since some of the molecule images were incorrectly numbered, and expanded the caption to make the contents of the figure clearer to the reader;
- Authors checked spectra data, biological, chemical data and supporting information.